

GROUP 4  
Downgraded at 3 year  
interval, declassified  
after 12 years



COPY 2

## TECHNICAL MEMORANDUM

X-723

REFERENCE

A STUDY OF LIQUID HYDROGEN IN ZERO GRAVITY

By Lewis E. Wallner and  
Shigeo Nakanishi

Lewis Research Center  
Cleveland, Ohio

LIBRARY COPY

SEP 13 1963

LEWIS LIBRARY, NASA  
CLEVELAND, OHIO

CLASSIFIED DOCUMENT - GROUP 4  
DECLASSIFIED  
By H. G. Maines  
Date 4-6-1972  
ser MR

CLASSIFIED DOCUMENT - GROUP 4, DECLASSIFIED

This document contains information which, if disclosed, could result in the United States Air Force being  
furnished with information, the disclosure of which, in any form, would be an unauthorized disclosure of information.

NATIONAL AERONAUTICS AND SPACE ADMINISTRATION  
WASHINGTON

August 1963

DECLASSIFIED

~~DECLASSIFIED~~  
NATIONAL AERONAUTICS AND SPACE ADMINISTRATION

TECHNICAL MEMORANDUM X-723

A STUDY OF LIQUID HYDROGEN IN ZERO GRAVITY\*

By Lewis E. Wallner and  
Shigeo Nakanishi

SUMMARY

The potential use of liquid hydrogen as an energy source for space applications raises new questions concerning the effects of weightlessness on this fluid. An extensive study of gravitational effects is being conducted at the Lewis Research Center with several types of test facilities including drop tower, airplane, ballistic rocket, and orbiting vehicles. Although a considerable amount of work must be done before hydrogen storage systems can be confidently designed for weightless environments, much new information has been uncovered as a result of these efforts. When surface-tension forces predominate, liquid hydrogen will initially wet the walls of its container and probably will not break into a mass of droplets. The position of the liquid can be influenced by capillary devices and the nucleate boiling heat transfer process is not significantly affected by changes in gravity.

The storage of liquid hydrogen in a space system was simulated by ballistic projection of a 9-inch-diameter vessel where about 5 minutes of weightlessness were obtained. The effects of weightlessness were complicated by the addition of inertial and heat-transfer forces. Although the liquid hydrogen at first wetted all the vessel walls, heat transfer to the closed container then started to dry the walls, which set up a thermal stratification pattern and resulted in abnormally high pressure rise rates. Agitation of the fluid did not destroy the thermal gradients but resulted in a considerable pressure rise as the fluid sloshed against the hot container wall. From tank outflow tests it was shown that liquid could be removed without serious distortion of the liquid-vapor interface but only with consideration given to flow velocity and vessel geometry. Direct application of liquid hydrogen research work on a small scale and for short weightless times is difficult because of the lack of adequate scaling understanding.

INTRODUCTION

The study of liquid hydrogen in zero gravity embraces a wide spectrum of problems, both fundamental and applied. Successful use of this propellant for space flight will necessitate sufficient experimentation and analysis to solve these unknowns, or at least to learn enough to permit designers to circumvent them. For illustrative purposes, consider such typical fundamental areas for in-

\*Title, Unclassified.

~~DECLASSIFIED~~

~~CONFIDENTIAL~~  
DECLASSIFIED

vestigation: heat-transfer coefficients at low flux levels; bubble mechanics, their motion and coagulation; liquid disposition, including location and control of the ullage space; fluid dynamics; damping rates; and sloshing characteristics. In the applied area there is the simultaneous action of many fundamental phenomena; but in addition, complex situations such as liquid positioning in zero gravity with heat addition and propellant outflow must be examined; or heat dispersion in a storage vessel where boiling is taking place at the wall, stratification within the fluid, vapor movement toward the liquid-gas interface and, finally, condensation.

The intrinsic nature of liquid hydrogen makes it a difficult fluid to study even though Lewis has a range of experience in this area dating back several years to the hydrogen propelled aircraft experiments (refs. 1 to 3). However, the task of exploring the zero-gravity effects on the fluid is especially complex because of the problem of simulating the weightless environment. The effects of gravitation on fluids have been theorized by many scientists such as Gauss, Dupré, and Rayleigh dating back over a century (refs. 4 to 6). Only recently have advances in high-speed photography, instrumentation, and test techniques permitted the observation of fluids in a weightless condition; that is, a 1-second period of weightlessness is simulated by dropping an experiment from a height of 16 feet. Experimental facilities have broadened from the linear free fall to include airplane, ballistic rocket, and orbital flight test techniques with an accompanying increase in zero-gravity test time from seconds to hours. A general perspective of the zero-gravity problems with respect to space power-plants together with a literature survey may be found in reference 7.

Early zero-gravity work at Lewis included photographic studies of boiling and capillary characteristics of a wetting fluid in a 9-foot free-fall facility (refs. 8 to 10), and boiling of liquid hydrogen for a 3/4-second weightless period in an open vessel (ref. 11). More recently, the completion of a 2.3-second drop tower, the launching of ballistic rocket experiments, and the fitting out of an airplane zero-gravity facility signaled the beginnings of a broader attack on the problems of weightlessness. With the help of these tools it has been possible to investigate, for example, the effect of contact angle, vessel shape, and filling on liquid position control in a weightless environment (ref. 12); the effectiveness of capillary control devices on liquid configuration with inertial and heat-transfer forces present (refs. 13 and 14); fluid outflow from a closed vessel; the dynamics of capillary pumping (refs. 14 and 15); and space storage of liquid hydrogen during 5 minutes of weightlessness with heat transfer (refs. 13 and 16). These and several other areas are being explored with the ultimate objective to be able to store and handle cryogenic fluids in a space environment.

Several incremental papers, which are indicated in the text and references, have been published concerning some of this work. Other publications that report individual studies are in process and many efforts are now in the performance and planning stages. The intent of the present work is to collect important aspects of much of the weightless experimentation, but primarily to indicate the interplay between the many facets of this complex field. Because the general understanding of weightlessness is still in an embryonic stage, it must be pointed out that some beliefs held valid today may subsequently be changed and that more critical problems may turn up than those envisioned in our present framework of knowledge.

~~CONFIDENTIAL~~  
DECLASSIFIED

CONFIDENTIAL  
DECLASSIFIED

A motion-picture film supplement C-223 has been prepared and is available on loan. A request card and a description of the film are given in the back of the report.

### TEST FACILITIES

As delineated in reference 7, there are generally three methods of observing fluids in a weightless environment, namely, in "drop" tower or linear free fall, parabolic airplane trajectory, and rocket propelled ballistic flight path. Description of such facilities can be found in references 12, 16, and 17. The time periods covered by these zero-gravity test techniques are in the 2-, 10-, and 300-second time regimes, at least for the experimentation described in the present paper. Aside from the obvious separation of test times, there are definite advantages and disadvantages that are associated with each of the zero-gravity facility types. These also are demonstrated in reference 7. Simply stated, zero-gravity studies in the drop tower can be conducted quickly and at a very low-gravity level, although the short test time limits both the size and complexity of the experimentation. Use of the airplane maneuver for zero-gravity work affords an increase in test time, but the difficulty of controlling the airplane makes testing considerably slower, less reproducible, and more expensive than in the drop tower. Only in the ballistic or orbital test technique can relatively long time zero-gravity experimentation be conducted; however, problems such as data telemetry and vehicle recovery result in test costs several orders of magnitude above that for either the drop tower or airplane facilities. Zero-gravity test results from all three facility types have been drawn upon for the present study. Sufficient duplication of experimentation has been conducted to assure that, where applicable, valid and interchangeable results from all three facility types can be obtained.

### RESULTS AND DISCUSSION

The considerable number of problems involved in the design of a cryogenic liquid system subjected to prolonged periods of weightlessness requires a many-sided approach. Effects of capillarity that are normally dismissed as negligible in a normal gravity environment become significant with decreasing "g" level and increasing system size.

Work conducted at Lewis has been aimed at obtaining a basic working knowledge of the behavior of liquids when capillary forces are made to prevail under laboratory controlled conditions. The synthesis of simplified problems into complex engineering application is sought with the intent of obtaining a clearer insight into the observed behavior of a typical cryogenic liquid system in space.

#### Fundamental Studies

Fluid configuration. - A basic question involved in the storage of liquid hydrogen in a zero-gravity environment is the disposition of liquid and vapor masses with respect to the tank. Estimation of heat transfer rates, effective

CONFIDENTIAL  
DECLASSIFIED

vehicle moment of inertia at impending orientation maneuver, and propellant pumping without vapor pullthrough are some of the considerations predicated on the knowledge of where the liquid exists at any given time. If all inertial forces and energy inputs are negligible, a totally wetting fluid will tend to spread over the container walls and a totally nonwetting fluid will tend to wet the smallest area, that is, form a sphere either tangent to the container or floating therein. The schematic representation in figure 1 shows the relation between contact angle and the probable fluid configuration. The totally wetting and totally nonwetting conditions are indicated by contact angles of  $0^\circ$  and  $180^\circ$ , respectively, with  $90^\circ$  being a neutral condition. An analytical development of fluid behavior embracing the concept of free surface energy in terms of the capillary area and the characteristic contact angle is given in reference 18. A modified derivation leading to the same basic result is also given in appendix A:

$$dE = \sigma_{l/v}(dA_{l/v} - \cos \theta dA_{l/s})$$

where

- E        system free surface energy
- $\sigma_{l/v}$     liquid to vapor interfacial tension
- $A_{l/v}$     liquid to vapor interfacial area
- $\theta$        characteristic contact angle
- $A_{l/s}$     liquid to solid interfacial area

This equation constitutes the basis from which many of the observed phenomena can be interpreted. An equally important concept is that of minimum potential energy, which says that the most stable equilibrium state of an isolated system of fixed mass is that state for which the internal potential energy is the least (ref. 18). If the system free surface energy is interpreted as this potential, a fluid system in the absence of gravitational or inertial forces will tend toward the state that constitutes the minimum. Qualitatively, this means that the energy increment  $dE$  must be negative for the assumed incremental change to occur. Results of carefully controlled experiments in thermal equilibrium reported in references 12 and 14 are in agreement with these concepts.

The possible applications of liquid hydrogen in aerospace technology have stimulated research in various areas related to this fluid in zero gravity. A prime requisite in predicting the behavior of liquid hydrogen is a knowledge of the characteristic contact angle. Despite the difficulties inherent in the measurement, results have been obtained (from information received in a private communication with Dr. Goode of Convair Astronautics) that seem to indicate a zero contact angle. Another source reported a contact angle other than zero (ref. 19); however, from the Aerobee tests conducted by Lewis, it was apparent that the liquid hydrogen wetted the walls of a spherical stainless-steel container after elimination of gravitational forces. Time histories of axial acceleration forces and wall temperatures of a 9-inch-diameter sphere 34 percent filled with liquid hydrogen during weightlessness are shown in figure 2. During the boost phase of

CONFIDENTIAL  
DECLASSIFIED

the trajectory, the acceleration forces collect the liquid hydrogen at the bottom of the container; the upper thermocouple records the hydrogen vapor temperature of about 110° R; the thermocouple at the bottom of the container reads the liquid hydrogen temperature of 37° R. At booster cutoff (time, 54 sec), the axial acceleration is reduced to zero and the liquid hydrogen quickly wets all the container walls, which results in uniform temperature readings. Although the initial wetting of the container walls was probably caused by inertial forces, the fact that they remained liquid wetted indicates that the contact angle was close to zero.

Reference 18 points out that a rigorous mathematical analysis of low-gravity hydrostatics for any but the simplest geometries is difficult because of the strong nonlinearity arising from the liquid-gas interface condition. If selected configurations are used, however, the physical manifestations of the underlying principles may be observed experimentally and compared with predicted behavior.

Some capillarity effects in confined liquids. - A specific demonstration of the tendency for system free surface energy to be minimized is reported in reference 14 and schematically shown in figure 3. A wetting liquid is placed in a cylindrical container that has a concentric tube within it. The tube diameter is varied to give a range of cylinder to tube radius ratio. The change in free surface energy as a function of change in liquid level in the tube can be written (derived in ref. 14)

$$dE = -2\pi \cos \theta \sigma_v / \lambda \left[ \frac{r \left( \frac{R}{r} \right)^2 - 2r - R}{\left( \frac{R}{r} \right)^2 - 1} \right] dh$$

where

E      free surface energy of system

$\theta$       contact angle

$\sigma_v / \lambda$       vapor to liquid interfacial tension

r      tube radius

R      cylinder radius

h      liquid-level height in tube

When  $R/r = 2$ , the quantity in the bracket is identically zero. When placed in zero gravity, there will be no fluid motion other than a minor meniscus change because the free surface energy of the system is already at a relative minimum. If the fluid column is displaced by some external means, the liquid mass will remain in the displaced position. The condition  $R/r = 2$  is thus a neutral point. When  $R/r > 2$ , the bracketed term is positive. Hence, for a change  $dh$  in the positive direction, there is a net decrease in free surface energy, that is, the liquid rises in the column. When  $R/r < 2$ , the bracketed term is negative.

CONFIDENTIAL  
DECLASSIFIED

DECLASSIFIED  
CONFIDENTIAL

Hence, for motion to proceed by virtue of a decreasing  $dE$ ,  $dh$  must occur in a negative direction. Thus, the liquid is depressed in the column and rises in the annulus.

If the same minimum energy principle is utilized, the liquid in a spherical vessel can be made to assume a predetermined position, as reported in reference 14. Shown in figure 4 is a spherical vessel containing a wetting liquid and a tube properly sized to meet the decreasing free surface energy requirement. Interconnecting holes permit liquid flow into the tube. Initially, the liquid assumes the normal 1-g configuration relative to the vertical regardless of tube location. In a zero-gravity condition, the free surface energy tends to become a minimum, and thus the tube is filled. A further movement toward a minimum is obtained when the external liquid wets the outer wall of the tube and distributes itself symmetrically about the tube axis. Because of weightlessness, a similar equilibrium configuration is expected for any tube location provided sufficient liquid and time exists for the entire liquid motion to occur. Evidence to this effect may be seen in figures 4(a) to (g) for the tube in the  $0^\circ$ ,  $45^\circ$ , and  $90^\circ$  positions. Thus, where all forces other than that of surface tension are near zero, a properly sized control tube may be used to position a fluid within a container.

Heat transfer. - The foregoing discussion has shown the relevance of some basic concepts to an understanding of fluid behavior in zero gravity. The presence of each input variable adds to the complexity and uncertainty of the problem. Determination of fluid behavior with heat addition and the possible effects of weightlessness on heat transfer become a major concern particularly in light of the cryogenic properties of liquid hydrogen.

The basic relation used in steady-state heat transfer is

$$\frac{\dot{Q}}{A} = h \Delta t$$

where

$\dot{Q}/A$  heat flux, Btu/(hr)(ft<sup>2</sup>)

$h$  heat-transfer coefficient, Btu/(hr)(ft<sup>2</sup>)(°R)

$\Delta t$  temperature difference, °R

Numerous dimensional studies and experimental correlations are found in the literature that express the heat-transfer coefficient in terms of geometry, fluid properties, and fluid dynamics parameters. These studies have similarly included the use of various definitions of temperature difference.

Experiments to assess the effects of zero gravity on heat transfer with liquid hydrogen are reported in reference 20. An electric heating element submerged in a hydrogen bath was used to measure the heat-input rate over a range of heater to liquid-bulk temperature difference. A transient technique with nitrogen in which a 1-inch-diameter copper sphere was utilized as a dynamic calorimeter was

DECLASSIFIED  
CONFIDENTIAL

CONFIDENTIAL  
DECLASSIFIED

reported in reference 21. The boiling heat transfer to liquid nitrogen at 1 atmosphere pressure was thus measured during free fall in a 32-foot drop tower. Results of the aforementioned investigations are shown in figure 5 for a heat flux range from  $2 \times 10^2$  to  $2 \times 10^4$  Btu per hour per foot squared for both 1-g and zero-gravity conditions. Boiling-water heat transfer under 1 g reported in references 8 and 22 also indicates the magnitude of temperature difference and heat flux. Reference 8 reported no effect of body force on the nucleate boiling process with water within the accuracy of the experiment. The agreement between the 1-g and zero-gravity data for all three liquids appears to be within the uncertainties of experimental error. Based on photographic observation of vapor cavities, the natural convection currents during the zero-gravity tests appear to be insignificant relative to the fluid motion induced at the boiling site (refs. 23 and 18). It may be concluded further that over the range of heat flux wherein comparable zero-gravity and 1-g heat-transfer data are available, and for the limited time scale of these experiments, the absence of natural convection had no significant effect on the local heat-transfer rate. This finding is in contrast to the expected effect of gravity on the boiling process as stated in reference 24, where it is postulated that the absence of a body force would result in a vapor blanket around the heated surface and thus sharply decrease heat-transfer rates.

Experimental boiling heat-transfer curves for liquid hydrogen from several other investigations are shown in figure 6. The theoretical curve of reference 25 based on a model embodying the dynamics of vapor cavities is shown to be consistent with experimental data in trend and magnitude. The analysis further indicated no influence of gravitational field on nucleate boiling heat transfer but considerable effect in the critical heat-flux region. Some of the scatter in the reference curves can be attributed to variations in experimental technique, apparatus, and test pressures, which ranged from  $3/4$  to about 2 atmospheres. The results of two Aerobee flight experiments are also seen to be within the general range of variables studied by the aforementioned investigators. The heat fluxes in these flights were approximately that received by a bare metal tank subject to direct solar radiation in space, as indicated in figure 6.

Practical considerations for storage of cryogenic liquids in space may require insulated tanks. Heat flux to a tank surrounded by a  $1/2$  inch of multi-layer foil-type insulation would be of the order of 0.25 Btu per hour per foot squared. In the investigation of reference 20, available zero-gravity time precluded observation of the nucleate boiling phenomenon below a heat-flux rate of about 200 Btu per hour per foot squared. Under normal gravity conditions, investigators generally observe a natural convection current whereby heat added to the liquid at the lower elevation is rejected at the upper liquid-vapor interface by surface evaporation. When heat is added at the top, temperature stratification occurs with heat conducted to the cooler liquid below (ref. 26). The relative significance of heat transfer by conduction only can be evaluated if a hypothetical layer of liquid hydrogen  $1/2$ -inch thick is assumed to receive a steady-state heat flux ranging from 0.1 to 10 Btu per hour per foot squared. The practical counterpart of such a model requires a continuous heat sink at the inner boundary with sufficient pressurization to suppress boiling. The change in thermal conductivity with temperature along the heat path was neglected. The nucleate boiling heat-transfer rate is two decades above that shown for the conduction process

CONFIDENTIAL  
DECLASSIFIED

DECLASSIFIED

at a given temperature difference. It is apparent that nucleate boiling would be necessary for the 100 Btu per hour per foot squared flux level of the Aerobee tests to maintain the temperature gradient at the 1° R level.

In summary, it may be said that the effect of weightlessness on heat transfer to liquid hydrogen is not clearly understood except by inference from observed results. In a zero-gravity condition if natural convection is assumed to be nonexistent, heat transfer by conduction may be a valid assumption provided the heat-flux rate is low and a continuous heat sink exists at the lower temperature boundary. In the absence of such a heat sink or at heat-flux rates above the stable conduction rate, conditions are attained by the liquid phase wherein boiling occurs. On a laboratory scale, isolated boiling experiments indicate little influence of body forces between zero gravity and 1 g on the heat-transfer mechanism at the boiling site, as attested by the heat-flux - temperature-difference relation. What is unknown, however, is the hydrodynamics of the vapor cavities and the surrounding liquid. A discussion of a possible model for this process, at least, in a 1-g field can be found in reference 27. Whereas vapor cavities are buoyed upward with resulting liquid agitation in 1-g pool boiling, or are swept away by the liquid flow velocity in forced convection tube boiling, the presence of neither mechanism in zero gravity requires a better understanding of the prevailing local hydrodynamics before the thermodynamic state of the entire system can be assessed. It is also possible that the stability of a liquid configuration based on free surface energy of an adiabatic fixed-phase system may be modified when another energy component such as heat is added accompanied by phase change.

Scaling. - The difficulty of subjecting full-scale systems to prolonged periods of weightlessness necessitates experimental investigations with scale models. Theory of models and the governing laws of similitude have been developed and widely applied to problems in the fields of hydro- and aerodynamics. The probable time scale of motion of fluids in a zero-gravity condition has been analyzed in references 18, 28, 29, and 30. The complexity of a general-configuration problem limited the analyses to order-of-magnitude-type studies. A general conclusion was that the time which characterizes the motion of liquids from one stable configuration to another was of the form

$$\tau = K \sqrt{\frac{\rho}{\sigma}} L^3$$

$\tau$  characteristic time

$\rho$  density

$\sigma$  surface tension

$L$  characteristic dimension

$K$  constant

The time scale for capillary fluid dynamics is thus based on  $\sqrt{(\rho/\sigma)L^3}$ . Reynolds (ref. 18) used a somewhat mechanistic approach in concluding that the

DECLASSIFIED

DECLASSIFIED  
CONFIDENTIAL

Reynolds, Bond, and Weber numbers are the principle dimensionless parameters encountered in low-gravity hydrodynamics and indicated the nature of phenomena to which each is applicable. Symbolically, these numbers are  $\rho v L / \mu$ ,  $\rho g L^2 / \sigma$ , and  $\rho v^2 L / \sigma$ , respectively, where

v velocity

$\mu$  viscosity

g gravitational acceleration

A simple manipulation of the Bond number and the equation for uniformly accelerated motion again yields the result that the time scale is proportional to the parameter  $\sqrt{(\rho/\sigma)L^3}$ .

For a given fluid, density  $\rho$  and surface tension  $\sigma$  are fixed, hence,  $\tau$  the characteristic time should vary as the characteristic length  $L$  raised to the  $3/2$  power. Hansen (ref. 30) calculated the oscillation period and decay time for liquid hydrogen and liquid nitrogen globules using the simplest oscillation mode (see appendix B). The results of this calculation are shown in figure 7(a), where the globule diameter (taken as the characteristic length) is shown as a function of the characteristic time. A single datum point is shown from an observed oscillation period of a liquid nitrogen globule photographed in the KC-135 airplane zero-gravity facility. The theory and data agree reasonably well for this one isolated point.

A wide gap exists, however, between the dynamics of a liquid confined in a space-vehicle tank and a free-floating globule of liquid. For the globule case, the characteristic time is interpreted as being proportional to the period of small oscillations about a spherical form. Considering the strong nonlinearity introduced by the liquid-vapor interface as it changes from a 1-g to a zero-gravity configuration, any agreement between the characteristic times of a tank configuration and the oscillating globule would be fortuitous and then only to perhaps a limited range of fluid motion. The extent of applicability of the given law of similitude to a more realistic tankage problem can be assessed by considering some results of tests reported in reference 12 that are shown in figures 7(b) and (c). The data are taken from a series of drop-tower tests with ethyl alcohol in spherical glass containers. The time to wet walls completely, that is, the period of weightlessness required for a wetting fluid to go from a 1-g configuration to a configuration in which the solid to vapor interface is seemingly replaced by a solid to liquid interface, is taken to be representative of a characteristic time for a liquid motion. The characteristic length is taken to be either (1) the spherical radius of the contained volume of liquid, or (2) the linear surface distance above the initial liquid level, that is, the total linear distance to be wetted. It should be noted that spherical containers with a given liquid- to tank-volume ratio result in tank radii that bear a direct relation to the spherical radii of the contained liquid. Furthermore, the radius of the tank raised to the  $3/2$  power varied as the square root of the tank volume. The line indicating the similarity law in figure 7(b) is therefore analogous to assumption (1).

DECLASSIFIED  
CONFIDENTIAL

DECLASSIFIED  
CONFIDENTIAL

From figures 7(b) and (c), it is apparent that neither liquid radius nor distance to be wetted sufficiently represents the characteristic length in the similarity function. Extrapolations based on the currently limited understanding of size and geometry effects on fluid dynamics can lead to considerable error when applied to tanks of space vehicle proportions. The full significance of this lack of scaling knowledge is difficult to assess at the present juncture.

From the preceding results, it is apparent that the present knowledge of scaling phenomena leaves much to be desired even for one of the simpler applications. Fluid motion whether induced by capillarity or external disturbances may be considered a reasonable certainty. Unsteady phenomena such as heat transfer into unvented tanks, variations in effective vehicle moment of inertia due to shifting of liquid mass, oscillations and sloshing effects as well as the hydrodynamics attending high rate influx and efflux of liquids give rise to partial differential equations whose complexity make scaling experiments greatly desirable.

#### Applied Studies

As stated previously, the physical properties of liquid hydrogen and the complexity of simulating a weightless environment make it difficult to study the zero-gravity effects on this fluid. As a result, much has been published regarding the likely action of hydrogen in such an environment based on heat transfer, surface tension, and fluid dynamic theory and some of the fundamental experimentation described previously (e.g., see refs. 31; 32, p. 156; and 33, p. 55). In this section an effort is made to illustrate typical results of some applied experimentation with liquid hydrogen that tend to shed new light on the zero-gravity characteristics of this fluid.

Uniform heating in a closed container. - A series of zero-gravity experiments have been performed by propelling a 9-inch-diameter spherical tank into a ballistic trajectory by means of an Aerobee sounding rocket, as described in reference 16. Flux rate, liquid filling, fluid collection, and heater location are some of the variables that have been examined. The heat-transfer vessel is shown in figure 8. Because of a lack of zero-gravity experimentation, heat transferred into a cryogenic storage tank in space has been generally assumed to be absorbed uniformly into the liquid (see refs. 23 and 32, e.g.). Thermal stratification in a normal 1-g environment with a cryogenic fluid is discussed in reference 26. By measuring the rise in pressure of the liquid hydrogen in the steel sphere as it was heated during several minutes of weightlessness, it was possible to determine the validity of the uniform heating assumption. For 200 seconds of zero gravity with a flux level of 150 Btu per hour per foot squared, the pressure changed from 15 to 85 pounds per square inch (fig. 9). From a calculation with thermal equilibrium within the liquid assumed, it was estimated that the pressure rise would have been only 60 pounds per square inch. From this test it was deduced that there was a considerable degree of thermal stratification within the fluid during heat addition in zero gravity. Such a condition was found to prevail for flux levels between 25 and 300 Btu per hour per foot squared and filling levels from 20 to 34 percent of the tank volume. At the point denoted fluid collection in figure 9, a collection rocket was fired which brought the liquid to

DECLASSIFIED  
CONFIDENTIAL

CONFIDENTIAL  
DECLASSIFIED

the bottom of the tank and resulted in the hydrogen sloshing against the container wall, part of which had dried off and became quite warm. Thus, a considerable amount of liquid hydrogen was vaporized. This rapid vaporization accelerated the rise in tank pressure though the heating rate was constant. At the point of separation of the experiment from the rocket, the fluid was sufficiently agitated to reduce the vessel pressure somewhat. Sufficient mixing would lower the pressure to the thermal equilibrium pressure line, as indicated in the figure.

A significant characteristic of hydrogen is the rapid change in pressure with increased liquid temperature, for example, between  $37^{\circ}$  and  $38^{\circ}$  R the equilibrium pressure rises 20 percent, from 15 to 18 pounds per square inch. Nevertheless, an attempt was made to measure the thermal stratification indicated by the pressure history in figure 9 by inserting a temperature measuring rake in the liquid hydrogen during a zero-gravity experiment. The resulting temperature profiles are shown in figure 10 for zero-gravity times from 0 to 200 seconds. During boost, the liquid is at the bottom of the container and a constant temperature profile of  $36.7^{\circ}$  R is indicated. At 30 seconds after sustainer rocket burnout, a maximum temperature profile of about  $1/2^{\circ}$  R was obtained. At 100 seconds of weightlessness the maximum temperature stratification is almost  $1^{\circ}$  R. This temperature profile then remains constant to a time of about 200 seconds after burnout. From these temperature readings, it is apparent that a thermal stratification is set up in a liquid hydrogen tank after a few seconds of weightlessness, and for the weightless time period of 200 seconds, the temperature profile is fairly stable once established.

The pressure rise of the liquid hydrogen storage vessel is plotted as a function of heat input for two heat fluxes and three tank fillings in figure 11. In the figure are shown calculated pressure rises for thermal equilibrium and tank fillings of 10, 30, and 50 percent. For most of the heat input range, the measured pressure rise corresponds to a liquid filling of about 15 percent for the thermal equilibrium calculation. At the higher heat inputs, the pressure is rising at a faster rate, which may be due to the hydrogen vaporization resulting from fluid collection or vessel tumbling near the termination of the flight. For the range of experimentation indicated, the danger in the design assumption of thermal equilibrium for a cryogenic storage vessel is apparent. For a tank heat input of 15 Btu (fig. 11) and a 34-percent liquid filling, thermal equilibrium would result in a pressure rise to about 65 pounds per square inch. With the measured stratification, an actual pressure of 85 pounds per square inch was obtained in the 9-inch-diameter spherical vessel used in the Aerobee experiments.

A comparison of the experimental data with the thermal equilibrium pressure rise, points up some very interesting questions; that is, for what extension in tank filling beyond 34 percent would the same experimental pressure rise be obtained? What level of heat flux rate will affect the tank pressure rise for a given heat input? What is the heat dispersion mechanism that accounts for the distinctive pressure rise rate?

Wall drying in zero gravity. - As indicated previously, surface tension forces would initially cause liquid hydrogen to wet the wall as gravity is reduced to zero; however, the addition of heat to the container brings other forces

CONFIDENTIAL  
DECLASSIFIED

CONFIDENTIAL  
DECLASSIFIED

to bear that can influence the position of the liquid. Unequal heat addition to a bubble or globule can result in its movement toward the higher temperature (see ref. 34). Concentrated heat leaks arising from vent lines or structure supports could raise the flux level to the boiling range, which would affect the fluid adjacent to the tank wall. In most of the Aerobee zero-gravity experiments, drying of the vessel walls occurred after a weightless period of from 150 to 200 seconds. This effect is illustrated in figure 12 where wall temperature traces are shown as a function of time for a 9-inch-diameter vessel 30 percent filled with liquid hydrogen with a uniform radiant heat flux of 150 Btu per hour per foot squared. Within a few seconds after burnout, the liquid hydrogen wets the walls and all thermocouples indicate readings close to the hydrogen saturation temperature. This state continues to time 220 seconds, (weightless time, 165 sec) where the top tank temperature rises rapidly, which indicates vapor wetting of the vessel wall in this area. The vapor-wetted-wall area grows in size until at 310 seconds the temperature near the vessel equator indicates liquid disappearance with the characteristic rise in temperature. The wall-drying inception generally starts in the vicinity of the liquid hydrogen fill tube and a camera viewing port (see fig. 8), where the heat flux has been estimated to be considerably higher than the 150 Btu per hour per foot squared shown for the data in figure 12.

In one of the Aerobee flights, definitive pictures were obtained of the wall-drying process as depicted in figure 13. In this particular experiment, the vessel was heated unsymmetrically with a flux level of 250 Btu per hour per foot squared on the lower hemisphere and about 1 Btu per hour per foot squared on the upper hemisphere, where the two halves are separated by an equator ring, as indicated in figure 13(a). The view in this figure is from the top of the container through a small window. The dark circle in the center of the picture is a ullage control device (similar to that shown in fig. 4), which was being investigated as a liquid-positioning vehicle, that operates by means of surface-tension forces. In figure 13(a), all the skin thermocouples around the sphere were reading liquid hydrogen temperatures. To the left of the equator ring, a bubbling pattern can be discerned that is representative of the nucleate boiling process. This would be expected from the flux level at 250 Btu per hour per foot squared, which is in the nucleate boiling range (fig. 6). At the bottom of figure 13(a), a light-colored region is outlined and is termed "intense boiling." The liquid film has probably thinned out here with a subsequent increase in the relative quantity of vapor bubbles in the liquid, which results in the greater opacity. That this intense-boiling area does not represent a transition to film boiling is shown by the data in figure 6, which indicates a minimum temperature difference of  $20^{\circ}$  R. Such a temperature difference is not shown by the temperature traces of figure 12 prior to the wall drying. Further evidence of this process is indicated in figure 13(b) where a small "dark" area appears in the middle of the intense boiling region (lower part of photograph) signifying the start of the wall-drying process. The wall temperature in this region increased rapidly at about the location of this dark area, which indicates the transition from liquid- to vapor-wetted wall. Progressive growth of the dry and intense boiling areas can be discerned in figure 13(c). In figure 13(d), the dark dry region has spread in an elongated pattern along the high flux side of the equator, and the evaporation process proceeds fast enough to release discernable clouds of hydrogen vapor. This drying process was traced by the change in wall temperature. In the lower portion of figure 13(d) the liquid-vapor interface at the vessel wall is stabilized. This

CONFIDENTIAL  
DECLASSIFIED

DECLASSIFIED  
CONFIDENTIAL

results from the increased surface-tension energy that tends to rewet the surface. The mechanics of this process will be subsequently analyzed in greater detail.

The rate at which the drying proceeds along the sphere and the possible effects of heat flux and liquid filling on the process are shown in figure 14 for uniform and nonuniform heating. Drying is indicated by a thermocouple located  $2\frac{1}{4}$  inches from the camera window, which is on the thrust axis, after a period of weightlessness of about 150 seconds. The drying then proceeds to the equator vicinity in about an additional 100 seconds (fig. 14(a)). Data for uniform heating flux of 260 and 150 Btu per hour per foot squared at liquid fillings of 22 and 34 percent, respectively, are shown. The curve faired through the drying data indicates a slowing down of the drying process in the vicinity of the equator. In another experiment, the 9-inch-diameter sphere was exposed to a nonuniform heat flux with the segmented heating elements symmetrical about the thrust axis. The wall drying seemed to emanate from the vicinity of the camera window in a time period similar to that obtained with the uniform heating (fig. 14). Three wall-temperature histories for the same nonuniform heating experiment are shown as a function of time in figure 15: one thermocouple is located close to the vessel top (about 3 in. from the thrust axis); each of the other thermocouples is near the equator, one in the middle of the "cold" wall (1 Btu flux) and the other in the middle of the "hot" wall (60 Btu flux). At burnout, the liquid quickly wets the wall at about 60 seconds after liftoff. The three thermocouples then reflect the slowly rising closed container pressure, which, of course, means an increase in liquid hydrogen temperature. Both the thermocouple near the fill tube at the top and at the equator in the low-flux zone show readings close to the saturation temperatures obtained from the vessel pressure. The equator thermocouple in the high-flux segment, however, reads about  $1^{\circ}$  R above the saturation temperature in the zero-gravity time between 75 and 180 seconds. It should be remembered though that this temperature difference exists at the wall, and because of the flux variation around the equator of the vessel the liquid-temperature gradient (from wall to liquid-gas interface) is probably not uniform. At about 180 seconds after liftoff, the thermocouple near the vessel top suddenly shows a rise in temperature indicating wall drying at that point (see fig. 15). At 240 seconds from liftoff, the drying region has spread toward the equator in the high-flux region. The drying did not proceed as far down the hemisphere with the low-flux heating, though it was seeded near the top of this area in the vicinity of the fill neck and camera window.

In figure 16, a plot of the liquid hydrogen temperature profile around the equator is shown for the experiment depicted in figure 15 at a time of 180 seconds from liftoff. All the temperatures shown reflect the uneven heating rate around the equator. The maximum temperature differential is  $1.5^{\circ}$  R.

In summary, some of the wall-drying characteristics are shown in the following table:

DECLASSIFIED  
CONFIDENTIAL

DECLASSIFIED  
CONFIDENTIAL

Test	Liquid hydrogen temperature, °R	Pressure, $\frac{\text{lb}}{\text{sq in.}}$ abs	Flux, $\frac{\text{Btu}}{(\text{hr})(\text{sq ft})}$	Vessel filling, percent	Zero gravity time for wall to dry, sec
1	44	42	260	22	150
2	47	60	150	34	150
3	40	25	<sup>a</sup> 25	30	170

<sup>a</sup>Unsymmetrical heating (average).

The interesting facet here is that even though the flux level, the vessel pressure, and filling have variations ranging to almost an order of magnitude, the zero-gravity time required for the wall drying to reach a particular location about 3 inches from the thrust axis was almost the same.

The transfer of heat into a cryogenic storage vessel is strongly dependent on the state of the fluid adjacent to the container walls. The Aerobee zero-gravity flight experiments have shown that an initially liquid-wetted wall invariably dried to form vapor-wetted regions despite the fact that the maximum heat-transfer rate (260 Btu/(hr)(sq ft)) was well below the film-boiling range (see fig. 6). This problem, therefore, was considered in greater detail. A spherical vessel is shown in figure 17 with a 30 percent filling of liquid hydrogen. As indicated previously, the likely shape of the ullage at equilibrium in zero gravity will also be spherical, and with no restraints the vapor bubble is free to move about the container at random with no change in surface-tension energy. The ullage is arbitrarily pictured at the top of the container in figure 17 so that the two spheres are tangent at this point. Attention is drawn to the relative shallowness of the liquid at the upper portion of the vessel.

Addition of heat into the thin film layer leads to the following postulated sequence of events:

(1) The liquid changes phase by nucleation in regions where the film has some minimum required thickness and by direct surface evaporation in regions of thinner films.

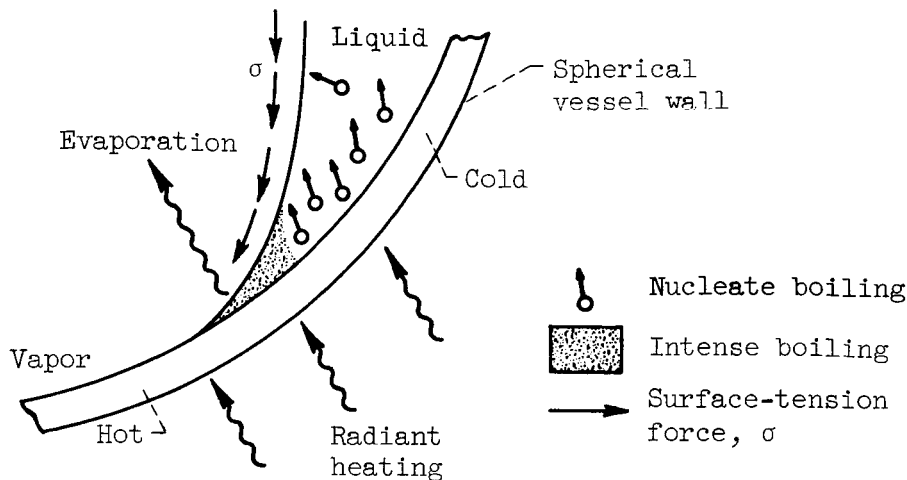
(2) As shown in appendix A, conversions from liquid-vapor to solid-vapor interfaces in thin films occur with almost no change in surface-tension energy. Hence, evaporation of a liquid film results in a vapor-solid interface with little or no tendency to rewet the wall.

(3) Once dried, the continued addition of heat causes a temperature rise in the container wall at a rate directly proportional to the heat input and inversely proportional to the thermal capacities and thermal conductivities of the wall and the vapor. The forces involved in this process are depicted in sketch (a).

Radiation heat energy is applied from a constant-temperature source. The cold-

DECLASSIFIED  
CONFIDENTIAL

CONFIDENTIAL  
DECLASSIFIED



(a)

wall region corresponds approximately to the saturation temperature (see fig. 12). The dry vapor-solid region of the wall is above the saturation temperature, which results in heat transfer by conduction along the wall as well as directly into the vapor. Where the liquid film is very thin, much of the radiative and conductive heat is absorbed by direct evaporation of the liquid hydrogen. Where the liquid film is sufficiently thick, the radiant heat transfer is absorbed into the fluid by the nucleate boiling process. The surface-tension force in a wetting liquid such as hydrogen tends to rewet the wall and thus replace the liquid evaporated in the heat-transfer process. Change in the vapor-wetted wall area depends on the relative balance between the heat transfer and the flow of liquid into the evaporative region arising from the surface-tension force.

The increase in surface-tension energy from the inception of the drying process was calculated for a vessel similar to the Aerobee Dewar with a 30-percent liquid filling, as is shown in figure 18. For simplicity, the calculation was limited to two dimensions, and the liquid-vapor interface was assumed to be circular. Where the liquid film is very thin, at the inception of the wall drying, the increase in surface-tension energy is quite small (fig. 18). As the dry region increases beyond about 2 radians, the surface-tension energy increases quite rapidly.

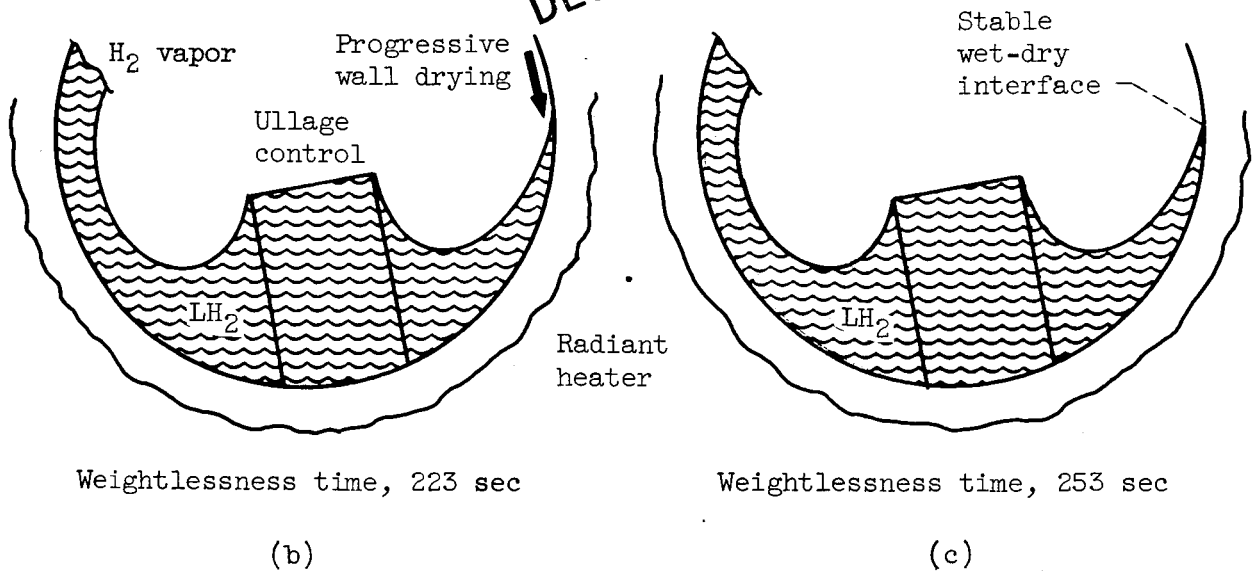
The rise in surface-tension energy and thus the tendency to rewet the dry wall helps to explain the slowing down of the drying process in the vicinity of the vessel equator with the Aerobee zero-gravity tests (see fig. 14). When the surface-tension energy is high enough to bring sufficient liquid into the evaporative region to balance the conduction and radiation heat input, the wet-dry interface would stabilize, and thus arrest the wall-drying process. Close examination of figures 13(c) and (d) indicates such a stabilization.

Sketches (b) and (c) made from the photographs in figure 13(c) and (d) between weightless times of 223 to 253 seconds indicate that the wall drying did not advance in the direction of increased surface-tension energy.

CONFIDENTIAL  
DECLASSIFIED

CONFIDENTIAL

DECLASSIFIED



From the evidence in sketches (b) and (c) and calculations of the wall-drying process in zero gravity, it is possible to construct the sequence of events in figure 19. (1) The energy-transfer process is depicted from the orderly nucleate boiling (fig. 19(a)), (2) to movement of ullage, which results in localized intense boiling (fig. 19(b)), (3) to the dry wall spot that appears because of the incapacity of thin liquid film to absorb heat input (fig. 19(c)), (4) to stabilization of wet-dry wall interface that results from high surface-tension forces circulating sufficient liquid to balance heat input from conduction and radiation (fig. 19(d)).

The partial drying of a cryogenic vessel in the absence of body forces is probably not peculiar to the results observed in these experiments. The extent of the drying in a zero-gravity field will be influenced by such factors as:

- (1) Restraint of vapor ullage
- (2) Heat-transfer process and associated fluid dynamics
- (3) Localized heat leaks
- (4) Fluid characteristics
- (5) Vessel shape

The importance of the wall drying will, of course, depend on the particular system being considered. It is probable, however, that the heat transfer, pressurization, and venting characteristics, for example, may be strongly affected.

Agitation of stratified fluid. - It has been postulated that miscellaneous perturbations resulting from such things as accelerations from trajectory corrections, pump vibrations, and equipment operation may preclude the formation of thermal gradients. Possible results from agitation of stratified fluid are indicated in figure 20. The curves represent a pressure rise of a fluid in a closed

CONFIDENTIAL  
DECLASSIFIED

CONFIDENTIAL  
DECLASSIFIED

container with and without thermal equilibrium. With sufficient agitation the pressure in a thermally stratified vessel might follow a path similar to AB (pressure drop resulting from mixing, which eliminated thermal stratification). Such a result was obtained in reference 26 for an experiment with liquid nitrogen in a 1-g environment. Near the end of two of the Aerobee zero-gravity flights, agitation of the fluid resulted not in a pressure drop but in a pressure rise, such as indicated by path AD in figure 20. The fluid in one experiment was agitated by tipping the vehicle end; in the other, collection rockets were fired, which drew the liquid hydrogen to the bottom of the vessel. At any rate, prior to the mixing, about one-half the area of the tank walls had dried and thus warmed above the liquid hydrogen temperature. When the liquid hydrogen moved up or splashed against the hot vessel wall ( $100^{\circ}$  to  $200^{\circ}$  R), there was immediate vaporization of some fluid resulting in a pressure rise above the normal stratified liquid path AC (fig. 20). Of course, after sufficient agitation, the tank pressure would return to a point on the thermal equilibrium line. The rise in pressure due to the vaporization of hydrogen is shown in figure 21 for the two Aerobee experiments previously mentioned. For the experiment in which the vehicle was tipped over until the telemetry measurements were cut off, an 18-percent rise in pressure was obtained, which represented a time period of about 20 seconds. In the experiment where the fluid collection rockets were fired, a 13-percent rise in pressure was obtained in 45 seconds. Additional mixing then sufficiently reduced the stratification in the liquid to effect a drop in tank pressure. From these data it would appear that thermal stratification of a cryogenic fluid in a weightless environment is not easily eliminated. After an initial disturbance of a stratified fluid in a partly dried tank, a considerable pressure rise is obtained as a result of the liquid sloshing up against the hot tank walls. From a calculation of the heat capacity of the dry vessel wall area, it was found that most of the heat was absorbed by evaporation of liquid hydrogen. In a pressurized tank design where vessel walls may be an order of magnitude heavier than those used in the present experiment, drying of the container walls would result in a proportionately greater pressure rise or venting requirement.

Effect of stratification, sloshing, and agitation. - Some of the possible zero-gravity effects on a fluid storage system can be illustrated by considering the previously discussed stratification, sloshing, and agitation phenomena in a closed vessel. Figure 22 indicates the pressure history of a cryogenic storage tank during vehicle coast with heat addition, engine prestart cycle, and engine firing. During the heat-addition period, the container pressure rises along the path AB for the idealized assumption of thermal equilibrium. The pressure does not change during the short prestart period BC. During engine firing, the idealized vessel pressure drops along path CD. In the actual case, heat addition in zero gravity is accomplished with thermal stratification, which would result in a higher pressure rise along path AF. The pressure at F is in excess of the maximum allowable as dictated by tank stress limit; and therefore the vessel would require venting along path EF to maintain the pressure within the maximum value. During the coast cycle it was assumed the vessel walls dried out in a manner similar to that obtained in the Aerobee experiments. Sloshing against the hot tank walls during the engine prestart cycle would result in an additional pressure rise represented by path FG as the liquid is vaporized. This would necessitate additional venting to keep the vessel pressure within the allowable limit. On engine firing then, the pressure would drop sharply, as along path GH, if the

CONFIDENTIAL  
DECLASSIFIED

DECLASSIFIED  
CONFIDENTIAL

resultant agitation was assumed to be sufficient to establish a condition of thermal equilibrium. Pressurization gas may now be required to restore the tank pressure to the level at C, to prevent too low a value being obtained during the engine firing cycle. The actual venting and pressurization requirements for large-scale storage systems arising from these zero-gravity effects are not known. However, from the trends indicated by the Aerobee experiments, major losses may result from fluid stratification, sloshing, and agitation in the zero-gravity environment.

The possible magnitude of propellant losses arising from storage in a weightless environment is illustrated by the following calculation: Assume that (1) a 9-inch-diameter sphere is (2) filled 35 percent with liquid hydrogen and is (3) heated to raise the pressure from 15 to 60 pounds per square inch for homogeneous mixing. The results are:

Venting loss due to thermal stratification resulting in excessive pressure rise (EF) (fig. 22), percent . . . . .	3.5
Venting loss due to pressure rise caused by liquid sloshing against the hot, dry container wall (FG) (fig. 22), percent . . . . .	1.7
Pressurization gas required by agitation and elimination of stratification (HC) (fig. 22), percent . . . . .	0.1
Total losses (based on propellant tank capacity), percent . . . . .	5.3

Liquid position control. - The foregoing discussion points out the relevance of liquid position within the tank to heat transfer, thermal stratification, and pressure rise. From the drop-tower investigation of surface-tension control devices described previously, indications were that a properly proportioned stand-pipe in a tank could be used to control the liquid position. Selected frames from a high-speed movie sequence are presented in figure 23, which shows the behavior of ethyl alcohol contained in a 5-inch-diameter cylindrical tank. The central tube diameter was less than one-half the tank diameter, which corresponds to a condition in which liquid rises in the tube (fig. 3). The time increment between successive frames is about 0.2 second.

Although details such as liquid-vapor interface and the graduated scale adjacent to the tank are not clear, it is evident that the liquid motion passed through distinct phases. In frame (b) where perceptible movement has already occurred, the initial phase was a formation of pronounced menisci both in the central tube and the annular region. The menisci and the thin film rising in the annular region appeared to reach the maximum of a slightly oscillatory motion in frame (c) and receded slightly in frame (d) as liquid began to rise in the tube. Frames (e) to (k) span the progressive rise of liquid in the tube with the formation of a slightly convex meniscus in the tube in frame (k). The kinetic energy of the moving liquid was sufficient to cause a reversal in the meniscus (from concave to convex) but apparently was not of sufficient magnitude to overcome the potential rise incurred should the liquid overflow. Termination of free fall was apparently reached in frame (l) accompanied by a rise in g-level sufficient to disturb the less stable annular meniscus, but insufficient to accelerate the liquid within the tube. At any rate, the movement of the liquid in the capillary tube was similar to that shown within the sphere in figure 4 where the dominant force is that of surface tension.

DECLASSIFIED  
CONFIDENTIAL

DECLASSIFIED  
CONFIDENTIAL

In an effort to simulate environmental conditions more closely with longer periods of weightlessness, similar experiments were repeated in an airplane maneuver and in a ballistic Aerobee rocket flight. In the airplane maneuver, about 10 seconds of low gravity were obtained, and in the Aerobee flight, several minutes of near-zero gravity were accompanied by heat transfer at the flux level of 250 Btu per hour per foot squared. Movie sequences taken of the airplane experiment are shown in figures 24 and 25. Two cylindrical tanks 5 inches in diameter with a convex hemispherical cap on one end, as viewed by the liquid, and a nearly conical dome on the other were half-filled with ethyl alcohol. The upper tank contained a central tube with a diameter of less than one-half the tank diameter. The lower, tubeless tank was used for comparison. A sketch is included to show the general shape and relative location of the two tanks. In both sequences, the tank axes were initially horizontal, a departure from the drop-tower experiment shown in figure 23, but analagous to a case shown in figure 4. Frames (a) and (b) of figure 24 correspond to the  $2\frac{1}{2}$ -g pullup maneuver prior to entering the zero-gravity trajectory (see ref. 35). Successive frames are approximately 1 second apart, and frames (c) to (i) are periods of decreasing gravity. An initial acceleration imparted to the system favored the movement of liquid toward the conical end of the tank. This initial acceleration was apparently of small magnitude inasmuch as the resulting motion damped out sufficiently to yield an essentially static configuration within 5 seconds, frames (j) to (o). This time is consistent with the analysis presented in reference 18. The flow of liquid into the central tube is clearly visible from frames (n) to (s).

A qualitative comparison between the upper and lower tanks in these frames shows little tendency for the central tube to position the external liquid in any way largely different from the tubeless tank. This configuration may be considered to be one of minimum free surface energy. The path of liquid motion from the 1-g to the final zero-gravity configuration is progressively decreasing in free surface energy, as shown by the broken line A in sketch (e) (p. 26). The filling of the tube is a further tendency toward a minimum taken along a path in which liquid is extracted from the surrounding layer thus thinning the layer but not pulling the liquid away from the walls. This would incur a rise in system free surface energy.

Results from another flight of the same experiment are shown in figure 25. The initial orientation and time scale were similar to those of figure 24. The path of energy change accompanying the liquid motion was apparently quite different. There existed no liquid layer connecting the tube and external liquid; and consequently, there was no flow of liquid into the capillary control tube. The convex hemispherical caps of both the upper and lower tanks remained uncovered (e.g., see frame (r)). Consideration of the free surface energy change leads to the conclusion that covering the hemispherical cap with a convex liquid layer involves a relatively larger increase in  $dA_l/v$  than the corresponding decrease in  $dA_l/s$ . The result is a relatively minimum condition in the change of system free surface energy, as shown by point B in sketch (e) (p. 26). The relative minimum condition was attained by both tanks in figure 25 resulting in a liquid configuration wherein the presence of the capillary tube had no effect.

A more realistic environmental experiment with the capillary control tube is

DECLASSIFIED  
CONFIDENTIAL

DECLASSIFIED  
CONFIDENTIAL

represented by its use in the 9-inch-diameter sphere in an Aerobee flight, as pictured in figure 26, where simultaneous inertia, surface-tension, and heat-transfer forces were present. In figure 26(a), the start of the weightlessness period, the liquid hydrogen is wetting all the walls of the spherical container, and the control device is almost empty. Liquid in the capillary control can be evidenced by reflections of light off the surface. Slight light reflections are visible in figure 26(b), after 48 seconds of zero gravity. After 194 seconds of weightlessness (fig. 26(c)), the capillary control device is about full, but all the container-wall temperature measurements still indicate liquid-wetted walls. Drying of the vessel walls first started at about 200 seconds of low gravity, which was somewhat longer than the time obtained in experiments without the capillary control device. Another experiment in the MA-7 orbital flight with a similar liquid-positioning device is described in reference 15, where alcohol was successfully controlled during most of the low-gravity time.

The results of the airplane and rocket experiments show that consideration of the system free surface energy leads to a clearer understanding of liquid behavior during weightlessness. The path along which the liquid motion and the accompanying change in system free surface energy occurs should not be neglected. Where the free surface energy decreases progressively from an initial level to a final level with no external disturbance, the path of motion may be unique, terminating at the absolute minimum. If the path has a relative minimum, motion ceases at this point above the absolute minimum. In the case of a nearly stationary condition in the variation of free surface energy such as curve C in sketch (e) page 26, liquid motion may be exceedingly slow without being absolutely static. A nearly stationary or relative minimum condition may be "jumped" by external disturbances beyond which a progressively decreasing energy path will lead toward an absolute minimum (see curve D in sketch (e) p. 26).

Propellant outflow. - Use of liquid hydrogen as a propellant will probably necessitate the ultimate emptying of the storage vessel. Initial outflow may be attempted in a low-gravity environment. An important consideration is the relative stability of the liquid-gas interface. Localized velocity gradients may result in inertial forces higher than surface-tension forces and thus propellant vapor pullthrough to the liquid pumps. Several liquid outflow experiments have been performed to shed light on such a potentially dangerous possibility. Results of some tests are shown in figures 27 to 29. Liquid discharge from a conical shaped 125-milliliter vessel through a 1/4-inch line during a zero-gravity simulation in a drop-tower test is pictured in figure 27. The liquid-vapor surface is not seriously deformed during the entire liquid discharge. A similar test in a 100-milliliter sphere with a cylindrical standpipe is pictured in figure 28 (configuration similar to that in fig. 4). At the initiation of the drop, the liquid nearly fills the standpipe and positions the remaining fluid at the vessel base (fig. 28, frames (b) to (i)). After 1.7 seconds of weightlessness the 1/4-inch discharge line is opened and distortion of the liquid-vapor interface is clearly evident in both the standpipe and the spherical base (fig. 28(j)). The relatively high velocity in the discharge line resulted in vapor pullthrough in figure 28(n). Preferential discharge of propellant from the standpipe or the sphere is a function of pressure differential, discharge velocity, and hole size at the base of the standpipe. At any rate, the design of such a space storage vessel would be governed by the liquid requirement for engine

DECLASSIFIED  
CONFIDENTIAL

DECLASSIFIED  
CONFIDENTIAL

firing and consequent gravity-field attainment, which would then position the fluid in the vessel. Liquid discharge from a model cylindrical storage tank is shown in figure 29 from a drop-tower experiment conducted at Convair Astronautics. The simulated flow requirement out of the model hydrogen storage vessel resulted in high localized velocity gradients, which set up inertial forces. Premature vapor pullthrough occurred, as is clearly evident in the figure. Because it was not possible to change either the flow rate or the tank geometry, it was necessary to resort to ullage rockets to control the liquid-vapor interface during the engine prestart sequence. From these experiments, it is apparent that a wetting fluid like liquid hydrogen can be discharged from a storage vessel in a low-gravity environment, but careful consideration must be given to vessel geometry and discharge velocities.

Fundamental and applied experimentation. - From the foregoing discussion, it is apparent that a considerable chasm exists between the study of fundamental and applied problems in a weightless environment. Separate examination of fluid characteristics in zero gravity such as heat transfer, surface tension, or flow dynamics can be quite misleading when an attempt is made to apply these results to a space vehicle where many combined forces are acting simultaneously. Evidence of this is apparent from work of other researchers as well as that performed at the Lewis Research Center. It may be appropriate to illustrate some examples of the fundamental zero-gravity experimentation and how the subsequent conclusions were altered in the light of additional applied studies. In the area of heat transfer, several experiments were performed that indicated decreasing bubble velocity during boiling as the gravity field was reduced (e.g., refs. 8 and 24). From this work, it was logical to reason that, in zero gravity, a vapor blanket would envelop any heated surface and the heat-transfer coefficients would change dramatically. In reference 20 with liquid hydrogen and in reference 21 with liquid nitrogen, it was demonstrated that this did not occur, but that, in effect, the nucleate boiling heat-transfer coefficients seemed to be independent of body forces. The data obtained in the Aerobee experiments appear to corroborate this finding. The lack of importance of the natural convective forces in the total heat-transfer process in zero gravity is discussed in references 18 and 20. However, the exact mechanism by which the heat is transported from the vessel wall to the liquid-gas interface is not clearly understood. At any rate, it has been inferred from the preceding discussion that knowledge that the walls will be liquid wetted and that the heat-transfer coefficients are not affected by body forces does not in itself permit an engineer to design a cryogenic storage system that will operate efficiently in a weightless environment. Some key facets were not realized until the attempt was made to store the liquid under several minutes of weightlessness simultaneously with the addition of heat. Only then were the thermal-stratification characteristic and the wall-drying tendency revealed.

Further evidence of the need for adequate environmental simulation is the proposal of the use of surface-tension forces as a solution for the liquid-positioning problem. Consideration of surface-tension theory and the minimum-energy principle led Ta Li (ref. 29) to propose the "standpipe" configuration as a means of controlling the ullage space. Similarly, experimentation in the Lewis 2-second drop tower led to the liquid-positioning device in figure 6. However, where boiling may create vapor pockets dispersed through the liquid or vehicle

DECLASSIFIED  
CONFIDENTIAL

DECLASSIFIED  
CONFIDENTIAL

orientation maneuvers result in inertial forces far greater than those of surface tension (ref. 31), reliance on such devices, without investigation under simultaneous action of all environmental conditions, must be weighed carefully. Further discussion may be found in reference 18, pages 35 and 36.

Environmental simulation. - Study of any space storage problem under conditions short of complete environmental simulation is going to require some extrapolation from a given level of understanding. This difficulty is illustrated in the following list, which is indicative of some factors that must be considered for the storage of a cryogenic fluid in a zero-gravity environment:

- (1) Size of experiment
- (2) Shape or geometry
- (3) Time
- (4) Heat flux level
- (5) Fluid disturbance
- (6) Vessel surface condition
- (7) Vessel filling
- (8) Fluid characteristics
- (9) Discharge of fluid
- (10) Vessel pressurization

Size of the experiment is mentioned first because it is perhaps the most obvious question that arises in trying to apply recent studies to space applications. Liquid hydrogen storage vessels with diameters as large as 30 feet are being contemplated; however, in a 1-second free-fall facility, zero-gravity research with liquid hydrogen limits the container size to the 1-inch regime (see fig. 8); the Aerobee nose cone limited the experiment to a 9-inch diameter. A considerable need exists for a method of extrapolating laboratory studies to more meaningful sizes. As indicated previously in the scaling discussion, the theory has been developed for scaling the oscillation or damping time of a spherical globule, although this work is largely unchecked. However, the method of scaling damping characteristics in a closed container, allowable acceleration of a free surface, or thermal stratification patterns, and many other questions are not understood in the small-scale regime in a weightless environment, much less the method of extrapolation to the large tank size.

The importance of test time becomes clear when one realizes that the majority of experimentation has been done in the 1-second area with a small effort in the minute regime by the use of sounding rockets. Effects of weightlessness on fluid storage for several days time in the lunar mission or several months time for the Mars mission must be understood before fluid storage systems can be de-

DECLASSIFIED  
CONFIDENTIAL

DECLASSIFIED  
CONFIDENTIAL

signed. The wall-drying and thermal-stratification phenomena could not have been observed in 1-second testing for example. What new problems may arise when the zero-gravity time is extended several orders of magnitude remains to be seen. However, long time weightlessness may not have as many problems as once supposed, for example, the concern that a liquid would ultimately break into many small droplets (ref. 36) may be unfounded, as evidenced by the orbital experiment described in references 15 and 37. The MA-7 spacecraft flight included a test that consisted of a 3.3-inch-diameter spherical vessel partly filled with a wetting fluid. In the low-gravity flight time in excess of 4 hours, the liquid-vapor interface was stable and the liquid configuration was similar to zero-gravity tests performed in the drop tower.

Related to the problem of zero-gravity test time is the heat-transfer level. Short test times necessitate high heat-flux levels in order that measurable temperature gradients are obtained. With the Aerobee-type experiment, the 3-minute zero-gravity time permits a heat-transfer level of perhaps 100 Btu per hour per foot squared with a resulting temperature gradient of  $1.0^{\circ}$  R (see fig. 10). For cryogenic storage on the lunar mission, with insulated tankage, for example, a flux level several orders of magnitude below this would be encountered. Initially, at least, the entire heat-transfer process would be altered with emphasis on the conduction instead of the boiling range (see ref. 38). To obtain meaningful measurements at such low heat-transfer levels would require weightlessness test times far longer than those presently obtainable.

A study of the motion pictures of the 9-inch-diameter spherical tank used in the Aerobee zero-gravity experiments seemed to indicate that currents of the forced-convection type may have been set up within the fluid as a result of the heat-transfer process. In addition, as discussed previously, liquid motion or perturbations present in the fluid could hinder the successful operation of a capillary control device for positioning the liquid in zero gravity. From the analysis represented in figure 7(a) and reference 18, many hours may be required to damp out fluid motion in a large tank existing in a weightless environment. However, the nature of the fluid motion arising from heat-transfer forces, for example, is not understood, much less the influence of geometry, size, or time on the process.

Conditions of the cryogenic storage vessel surface can have important effects on the weightless characteristics of fluids. In reference 39, it is demonstrated that surface cleanliness can have an order-of-magnitude effect on the heat-flux levels obtained for liquid hydrogen at a given temperature difference. Tests in the drop tower and the Aerobee rocket indicate liquid hydrogen exhibiting characteristics of a wetting fluid. Yet in reference 19, the contact angle was measured to be  $80^{\circ}$  to  $90^{\circ}$ , a near neutral value. It is felt that surface condition must play an important part in these results. The profound effect that contact angle can have on the zero-gravity configuration of a fluid is delineated in reference 12.

As indicated in reference 39, the heat input to the fluid for a given heat load on the spherical container walls varies directly with the diameter. However, as thermal equilibrium probably does not exist in a zero-gravity environment, the heat-transfer characteristics will be strongly affected by the ullage

DECLASSIFIED  
CONFIDENTIAL

CONFIDENTIAL  
DECLASSIFIED

(see ref. 36). With greater liquid filling, results of the present study indicate that the liquid-gas interface condition will cause a larger deviation from the thermal equilibrium assumption. This can result in heavier venting and pressurization requirements. In addition, the degree of filling can affect the weightless configuration of the fluid (ref. 12), drying of the vessel walls, damping characteristics, vapor entrainment, and so forth.

From the foregoing discussion then it is apparent that a number of factors must be considered to perform definitive experimentation of liquid hydrogen in a zero-gravity environment.

#### SUMMARY OF RESULTS

Zero-gravity studies of liquid hydrogen and other wetting fluids have led to several conclusions regarding the use of this propellant for space applications. Where intermolecular forces are dominant, liquid hydrogen will initially wet the walls of its container and probably remain in a homogeneous mass instead of breaking into droplets even on long time exposure to low gravity. The position of the liquid can be influenced by capillary devices, and the nucleate boiling heat transfer process is not significantly affected by natural convection. Use of liquid hydrogen in a space storage system, however, can be complicated by the addition of inertial or heat-transfer forces, for example. Heat transfer to a closed container started to dry the liquid hydrogen wetted walls in a relatively short time period. The heating process resulted in thermal stratification and an abnormally high pressure-rise rate. Agitation of the fluid did not destroy the thermal gradients but did result in a considerable pressure rise as the cold hydrogen sloshed against the hot container wall. From tank outflow tests, it was demonstrated that a vessel could be emptied of liquid without serious distortion of the liquid-vapor interface, but only with consideration given to flow velocity and vessel shape.

Direct application of the liquid hydrogen research work to system design is difficult because of the lack of adequate scaling understanding. The need for scaling from model and short time studies to large-scale vessels for the long weightlessness times is especially acute because of the difficulty of zero-gravity environmental simulation. From these experiments, it has become clear that careful design efforts will be required for the successful storage and handling of liquid hydrogen in a low-gravity environment.

Lewis Research Center  
National Aeronautics and Space Administration  
Cleveland, Ohio, March 14, 1963

CONFIDENTIAL  
DECLASSIFIED

CONFIDENTIAL  
DECLASSIFIED

## APPENDIX A

### FREE SURFACE ENERGY THEORY

The free surface energy of a system consisting of liquid to vapor, vapor to solid, and liquid to solid interfaces may be written as

$$E = \sigma_{l/v} A_{l/v} + \sigma_{v/s} A_{v/s} + \sigma_{l/s} A_{l/s} \quad (A1)$$

where

$E$  system free surface energy

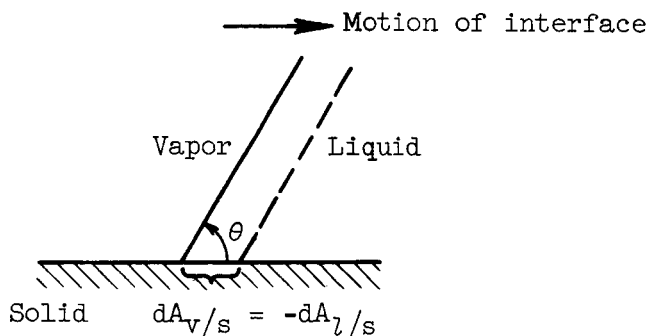
$\sigma_{l/v}, \sigma_{v/s}, \sigma_{l/s}$  liquid to vapor, vapor to solid, and liquid to solid interfacial tensions, respectively

$A$  interfacial area

For a virtual change of incremental size,

$$dE = \sigma_{l/v} dA_{l/v} + \sigma_{v/s} dA_{v/s} + \sigma_{l/s} dA_{l/s} \quad (A2)$$

From physical reasoning, a moving liquid to vapor interface establishes the condition  $dA_{v/s} = -dA_{l/s}$ .



(d)

Substituting and collecting terms yield

$$dE = (\sigma_{l/s} - \sigma_{v/s}) dA_{l/s} + \sigma_{l/v} dA_{l/v} \quad (A3a)$$

or

$$\frac{dE}{\sigma_{l/v}} = \left( \frac{\sigma_{l/s} - \sigma_{v/s}}{\sigma_{l/v}} \right) dA_{l/s} + dA_{l/v} \quad (A3b)$$

CONFIDENTIAL  
DECLASSIFIED

CONFIDENTIAL  
DECLASSIFIED

From Dupré's equations,

$$\frac{\sigma_{l/s} - \sigma_{v/s}}{\sigma_{l/v}} = -\cos \theta \quad (A4)$$

where  $\theta$  is the characteristic contact angle. Therefore,

$$dE = \sigma_{l/v}(dA_{l/v} - \cos \theta dA_{l/s}) \quad (A5)$$

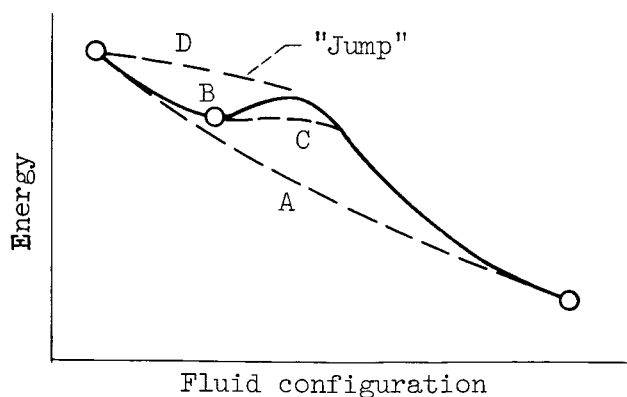
For the fluid configuration to change, it is required that  $dE$  be negative, or decreasing. When a liquid is totally wetting ( $\cos \theta = 1$ ), motion of the liquid can proceed as long as  $dA_{l/s} > dA_{l/v}$ .

When a liquid is totally nonwetting ( $\cos \theta = -1$ ), liquid motion proceeds along a path that yields a net decrease in the liquid to vapor and liquid to solid interface areas.

When  $\cos \theta = 0$ , the liquid to solid interface is immaterial. The path of liquid motion tends to minimize the liquid to vapor interface with the interface contacting the solid surface at right angles.

A schematic diagram of the system free surface energy as a function of fluid configurations may be shown along various paths as follows:

- (1) A progressively decreasing path A defines a unique absolute minimum.



(e)

- (2) A relative minimum path B can inhibit further configuration changes toward the absolute minimum.

- (3) A nearly stationary condition as shown by path C results in exceedingly slow motion.

It is interesting to note that thin spreading films of a totally wetting liquid

CONFIDENTIAL  
DECLASSIFIED

CONFIDENTIAL  
DECLASSIFIED

( $\cos \theta = 1$ ) yield the condition where  $dA_{l/v} \approx dA_{l/s}$ : from equation (A5), such a condition leads to  $dE \rightarrow 0$  or nearly stationary motion.

External disturbances, kinetic energy, or other energy inputs could force the fluid configuration to "jump" beyond the relative minimum or nearly stationary condition thus permitting fluid motion to reach the absolute minimum.

In the absence of energy inputs, fluid motion that tends to raise the system free surface energy is not possible.

DECLASSIFIED  
CONFIDENTIAL

CONFIDENTIAL  
DECLASSIFIED

## APPENDIX B

### SOME THEORY OF SCALING

Analysis of the motion of liquids in zero gravity becomes difficult because the liquid has complete mobility unconstrained by gravitational forces and a confining boundary along the liquid-vapor interface. For a closed system in a weightless environment, energy functions such as surface convolutions, heat input, friction, random accelerations, and small sustained accelerations have relatively significant effects on the overall liquid motion.

The period of oscillation of fluid globules has been derived in reference 40 to be

$$T = \pi \sqrt{\frac{[(n+1)f_g + nf_s]r^3}{2n(n+1)(n-1)(n+2)}}$$

where

$$f_g = \frac{\rho_g}{\sigma}$$

$$f_s = \frac{\rho_s}{\sigma}$$

$\rho_g$  density of fluid in globule

$\rho_s$  density of fluid surrounding globule

$\sigma$  interfacial tension between fluids

The term  $\sqrt{(\rho/\sigma)r^3}$  is the basis for the similarity law of capillary fluid dynamics where  $r$  is a characteristic length (ref. 28). The higher harmonics of oscillation are accounted for by the  $n$  terms with  $n = 2$  corresponding to the simplest mode. For small perturbations about the spherical shape, the kinetic energy and free surface energy can be written or expanded in terms of the spherical radius. Hence, for the present case, the characteristic dimension is the radius.

Hansen made a determination of the motion of a column of liquid in a tube under zero-gravity conditions (ref. 30). The force-balance equation is written as

$$\frac{\pi}{4} d^2 \rho \ddot{Z}Z + \frac{\pi}{4} d^2 \rho \dot{Z}^2 + 8\pi\mu Z\dot{Z} = \pi d\sigma$$

where

CONFIDENTIAL  
DECLASSIFIED

CONFIDENTIAL  
DECLASSIFIED

- d tube diameter
- $\rho$  liquid density
- $\mu$  absolute viscosity of liquid
- Z length of liquid column

The first two terms of the left member are an expansion of the momentum term  $d(mv)/dt$  and the third term is the viscous force for assumed laminar flow. The right member is the surface-tension force. A solution of this equation for the flow velocity  $\dot{Z}$  is

$$\dot{Z} = \frac{\frac{8\sigma\tau}{\rho d} (1 - e^{-t/\tau})}{2 \sqrt{Z_0^2 + \left(\frac{8\sigma\tau}{\rho d}\right) [t - \tau(1 - e^{-t/\tau})]}}$$

where

- t time
- $\tau = \rho d^2 / 32\mu$
- $Z_0$  initial length of liquid column

The significant result of this analysis was that for a given tube size  $d$  the velocity nearly approached a constant as observed in experiments. If the viscous term is neglected, the solution for  $\dot{Z}$  simplifies to

$$\dot{Z} = \frac{4\sigma}{\rho d} \frac{t}{Z}$$

Solving this equation for  $Z$  yields

$$Z = \sqrt{\frac{4\sigma}{\rho d} t^2 + Z_0^2}$$

If  $Z_0$  is assumed to be zero for convenience because it affects  $Z$  at most by a constant,

$$Z = 2 \sqrt{\frac{\sigma}{\rho d}} t$$

which is a linear function in time.

For a given fluid in a given tube size, the linearity of  $Z$  with time indicates a constant velocity, proportional to the square root of  $\sigma/\rho d$ .

Examination of the equation would indicate that the flow velocity,  $Z$ , can

CONFIDENTIAL  
DECLASSIFIED

DECLASSIFIED  
CONFIDENTIAL

increase indefinitely as  $d$  is decreased. Physically, with decreasing tube size, viscous forces become no longer negligible such that a maximum corresponding to a finite tube size is obtained.

The same equation of motion can be derived directly by the methods of analytical dynamics. In systems where liquid flowing into a tube from a reservoir imparts considerable momentum to the reservoir fluid or where flow is accompanied with friction and heat transfer, the equation will be altered considerably from the conservative case.

The similarity laws generally derived from dimensional considerations defines a characteristic time in terms of

$$T = f \left( \sqrt{\frac{\rho L^3}{\sigma}} \right)$$

where  $L$  is a characteristic length (ref. 30).

If the equation for flow in a tube is solved for  $t$  to yield a "characteristic" time  $\bar{t}$  required to fill a given length,  $\bar{Z}$ ,

$$\bar{t} = \frac{\bar{Z}}{2} \sqrt{\frac{\rho}{\sigma}} d$$

Dimensionally this yields again

$$T = f \left( \sqrt{\frac{\rho L^3}{\sigma}} \right)$$

As in the equation for the oscillation period of a liquid globule, the length dimension appears to the third power. The parameter designated by  $L$  in the liquid column analysis, however, is neither  $d$  nor  $Z$  exclusively. This demonstrates the necessity of defining the liquid behavior in terms of a system function or, if possible, a dimension characteristic of the system function and its variation along the path of motion. Unlike homologous models in hydrodynamics, the unconstrained motion of liquids in zero gravity is probably not amenable to analysis by dimensional similarity alone.

DECLASSIFIED  
CONFIDENTIAL

DECLASSIFIED  
CONFIDENTIAL

#### REFERENCES

1. Silverstein, Abe, and Hall, Eldon W.: Liquid Hydrogen as a Jet Fuel for High-Altitude Aircraft. NACA RM E55C28a, 1955.
2. Ordin, P. M., Weiss, S., and Christenson, H.: Pressure-Temperature Histories of Liquid Hydrogen Under Pressurization and Venting Conditions. Vol. 5 of Advances in Cryogenic Eng., K. D. Timmerhaus, ed., Plenum Press, 1960, pp. 481-486.
3. Kerslake, W. R., and Dangle, E. E.: Tests with Hydrogen Fuel in a Simulated Afterburner. NACA RM E56D13a, 1956.
4. Dupré, Athanase: Memoirs of the Mechanical Theory of Heat. Nos. 5, 6, and 7, Ann. Chim. et de Phys., 1866-1868.
5. Rayleigh: Collected Scientific Papers. Vol. VI. Cambridge Univ. Press (London), 1920.
6. Young, Thomas: Essay on the Cohesion of Fluids. Roy. Phil. Trans., Dec. 20, 1805, pp. 65-87.
7. Unterberg, Walter, and Congelliere, James: Zero Gravity Problems in Space Powerplants: A Status Survey. ARS Jour., vol. 32, no. 6, June 1962, pp. 862-871.
8. Usiskin, C. M., and Siegel, R.: An Experimental Study of Boiling in Reduced and Zero Gravity Fields. Paper 60-HT-10, ASME-AIChE, 1960.
9. Siegel, R.: Transient Capillary Rise in Reduced and Zero Gravity Fields. Jour. Appl. Mech. (ASME Trans.), ser. E, vol. 28, no. 2, June 1961, pp. 165-170.
10. Usiskin, C. M., and Siegel, R.: An Experimental Study of Boiling in Reduced and Zero Gravity Fields. Weightlessness - Physical Phenomena and Biological Effects, Elliot T. Benedikt, ed., Plenum Press, 1961, pp. 102-110. (See also Jour. Heat Transfer (ASME Trans.) ser. C, vol. 83, no. 3, Aug. 1961, p. 243.)
11. Brazinsky, Irving, and Weiss, Solomon: A Photographic Study of Liquid Hydrogen Under Simulated Zero Gravity Conditions. NASA TM X-479, 1962.
12. Petrash, Donald A., Zappa, Robert F., and Otto, Edward W.: Experimental Study of the Effects of Weightlessness on the Configuration of Mercury and Alcohol in Spherical Tanks. NASA TN D-1197, 1962.
13. McArdle, Jack G., Dillon, Richard C., and Altmos, Donald A.: Weightlessness Experiments with Liquid Hydrogen in Aerobee Sounding Rockets; Uniform Radiant Heat Addition - Flight 2. NASA TM X-718, 1962.

DECLASSIFIED  
CONFIDENTIAL

DECLASSIFIED  
CONFIDENTIAL

14. Petrash, Donald A., Nelson, Thomas M., and Otto, Edward W.: An Experimental Study of the Effect of Surface Energy on the Liquid-Vapor Interface Configuration During Weightlessness. NASA TN D-1582, 1963.
15. Petrash, Donald A., Nussle, Ralph C., and Otto, Edward W.: Effect of the Acceleration Disturbances Encountered in the MA-7 Spacecraft on the Liquid-Vapor Interface in a Baffled Tank During Weightlessness. NASA TN D-1577, 1963.
16. Knoll, Richard H., Smolak, George R., and Nunamaker, Robert R.: Weightlessness Experiments with Liquid Hydrogen in Aerobee Sounding Rockets; Uniform Radiant Heat Addition - Flight 1. NASA TM X-484, 1962.
17. Hansen, J. L., and Perkins, C. R.: Zero-G Report - Flight Test Development. Rep. 55D-859-4, Convair Astronautics, May 21, 1962.
18. Reynolds, William C.: Hydrodynamic Considerations for the Design of Systems for Very Low Gravity Environments. Rep. LG-1, Stanford Univ., Sept. 1, 1961.
19. Anon.: Liquid Propellant Losses During Space Flight. Rep. 63270-00-03, Combined Third and Fourth Quarterly Prog. Rep. June 1-Nov. 30, 1961, Arthur D. Little, Inc., 1961.
20. Aerophysics Group: June-August Progress Report for the Combined Laboratory and KC-135 Aircraft Zero G Test Program. Rep. AE61-0871, Convair Astronautics, Sept. 5, 1961.
21. Merte, H., and Clark, J. A.: Boiling Heat-Transfer Data for Liquid Nitrogen at Standard and Near-Zero Gravity. Vol. 7 of Advances in Cryogenic Eng., K. D. Timmerhaus, ed., Plenum Press, 1962, pp. 546-550.
22. Forster, K. E., and Greif, R.: Heat Transfer to a Boiling Liquid; Mechanism and Correlations. Paper 58-HT-11, ASME, 1958.
23. Burry, Roger: Liquid Propellant Storage in Earth Satellite Orbits. Rocketdyne, North Am. Aviation, Inc., 1960.
24. Westwater, J. W.: Things We Don't Know About Boiling Heat Transfer. Dept. Chem. and Chem. Eng., Univ. Ill.
25. Drayer, D. E., and Timmerhaus, K. D.: An Experimental Investigation of the Individual Boiling and Condensing Heat-Transfer Coefficients for Hydrogen. Vol. 7 of Advances in Cryogenic Eng., K. D. Timmerhaus, ed., Plenum Press, 1962, pp. 401-412.
26. Huntley, Sidney C.: Temperature-Pressure-Time Relations in a Closed Cryogenic Container. NACA TN 4259, 1958.
27. Hsu, Yih Yun, and Graham, Robert W.: An Analytical and Experimental Study of the Thermal Boundary Layer and Ebullition Cycle in Nucleate Boiling. NASA TN D-594, 1961.

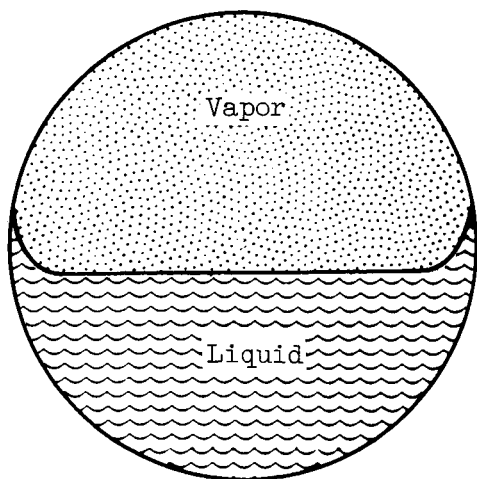
DECLASSIFIED  
CONFIDENTIAL

DECLASSIFIED  
CONFIDENTIAL

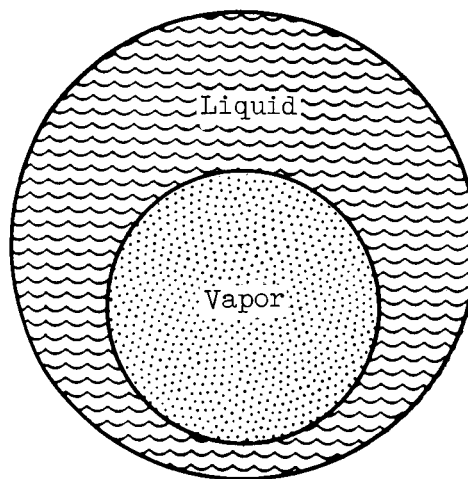
28. Benedikt, E. T., ed.: Weightlessness - Physical Phenomena and Biological Effects. Plenum Press, 1961.
29. Li, T.: Cryogenic Liquids in the Absence of Gravity. Vol. 7 of Advances in Cryogenic Eng., K. D. Timmerhaus, ed., Plenum Press, 1962, pp. 16-23.
30. Hansen, J. L., and Wood, G. B.: Liquid Oscillations and Damping. Rep. 562-1-550, Convair Astronautics, Apr. 25, 1961.
31. Neiner, J. J.: The Effect of Zero Gravity on Fluid Behavior and System Design. TN 59-149, WADC, Apr. 1959.
32. Shaffer, A., ed.: Analytical Methods for Space Vehicle Atmospheric Control Processes, pt. I. ASD Tech. Rep. 61-162, AiResearch Mfg. Co., The Garrett Corp., Oct. 1961.
33. Hammer, Lois R.: Aeronautical Systems Division Studies in Weightlessness: 1959-1960. TR 60-715, WADC, Dec. 1961.
34. Young, N. O., Goldstein, J. S., and Block, M. J.: The Motion of Bubbles in a Vertical Temperature Gradient. Jour. Fluid Mech., vol. 6, pt. 3, Oct. 1959, pp. 350-356.
35. Schwartz, E. W.: Liquid Behavior Investigations Under Zero and Low G Conditions. Convair Astronautics, 1962.
36. Satterlee, H. M.: Propellant Control at Zero G. Space/Aero., vol. 38, no. 1, July 1962, pp. 72-75.
37. Kolcum, Edward H.: Next Astronaut May Spend 3 of 6 Orbits in Drift Flight. Aviation Week, vol. 76, no. 23, June 4, 1962, pp. 26-30.
38. Olivier, J. R., and Dempster, W. E.: Orbital Storage of Liquid Hydrogen. NASA TN D-559, 1961.
39. Class, C. R., DeHaan, J. R., Piccone, M., and Cost, R. B.: Boiling Heat Transfer to Liquid Hydrogen from Flat Surfaces. Vol. 5 of Advances in Cryogenic Eng., K. D. Timmerhaus, ed., Plenum Press, 1960, pp. 254-261.
40. Lamb, Horace: Hydrodynamics. First Am. ed., Dover Pub., 1945.
41. Merino, F.: Simulation of and Recommendations for Centaur Vehicle Pre-Start and Chillumdown Flow Sequences. Rep. AY62-0013, General Dynamics/Astronautics, Aug. 2, 1962.
42. O'Hanlon, T. W.: Liquid Hydrogen Film Boiling. Convair Astronautics, 1962.

DECLASSIFIED  
CONFIDENTIAL

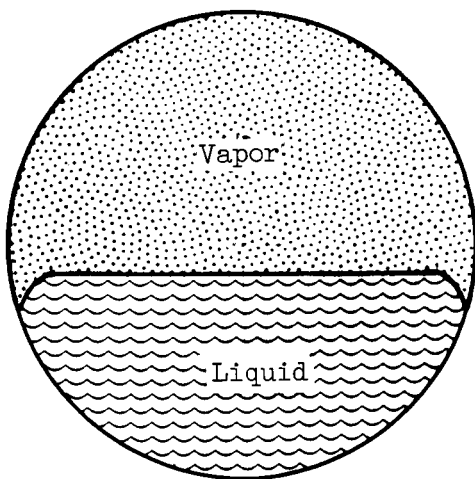
DECLASSIFIED  
CONFIDENTIAL



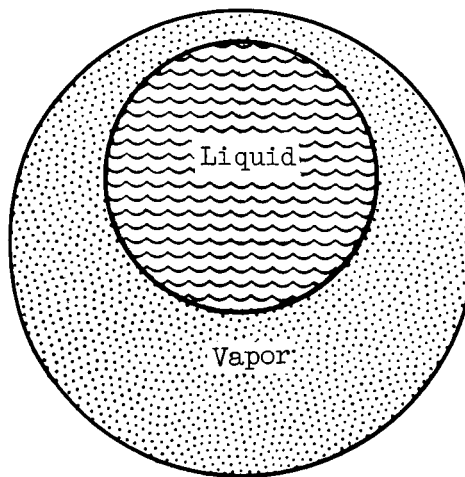
(a) 1-g configuration  
of wetting fluid.



(b) Zero-gravity configuration  
of wetting fluid.



(c) 1-g configuration  
of nonwetting fluid.

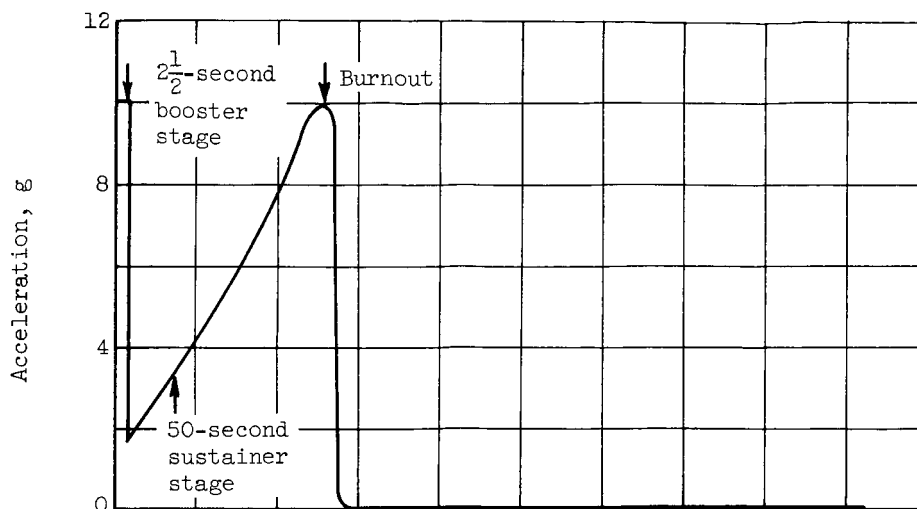


(d) Zero-gravity configuration  
of nonwetting fluid.

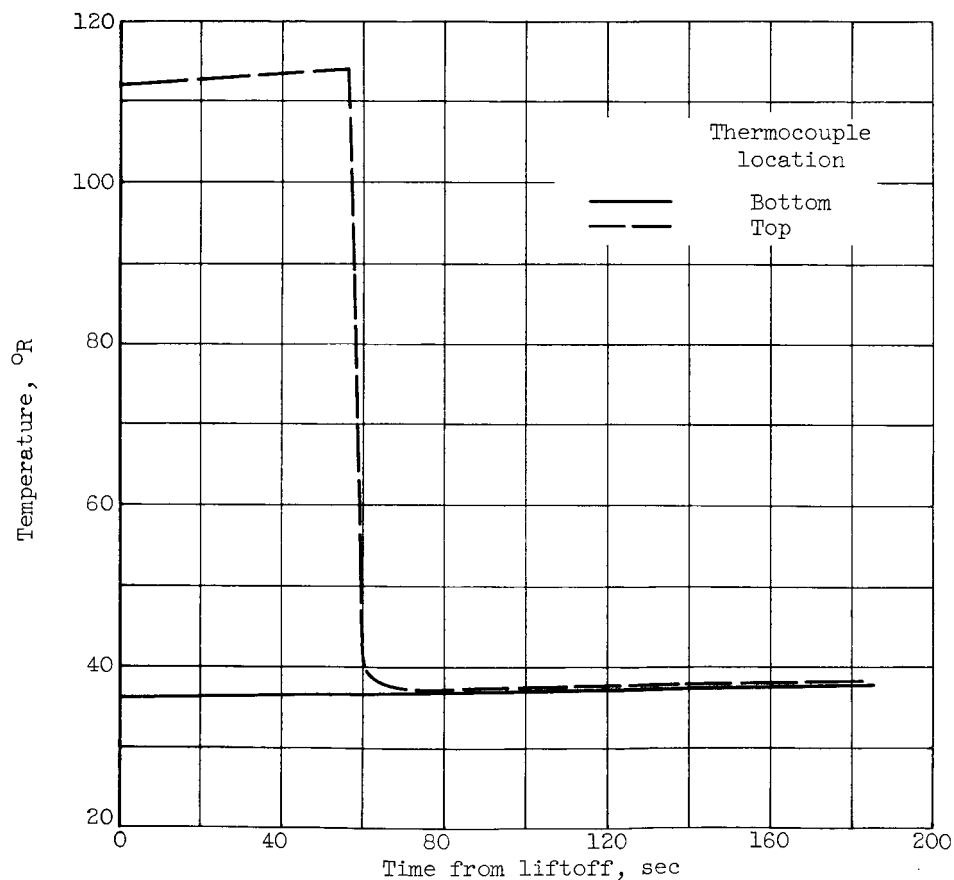
Figure 1. - Disposition of wetting and nonwetting fluids in 1 g and zero gravity. (See ref. 12 for discussion of contact angles.)

DECLASSIFIED  
CONFIDENTIAL

DECLASSIFIED  
CONFIDENTIAL



(a) Vessel acceleration.

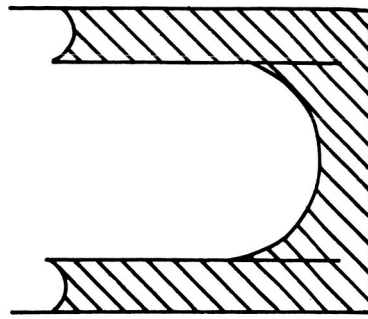


(b) Vessel wall temperature.

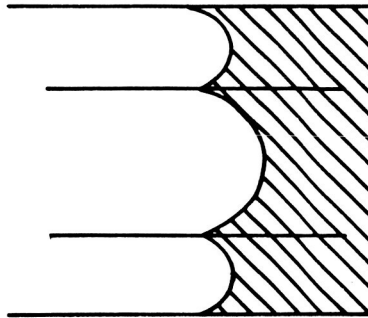
Figure 2. - Acceleration and wall-temperature history of 9-inch-diameter stainless-steel sphere 34 percent filled with liquid hydrogen.

DECLASSIFIED  
CONFIDENTIAL

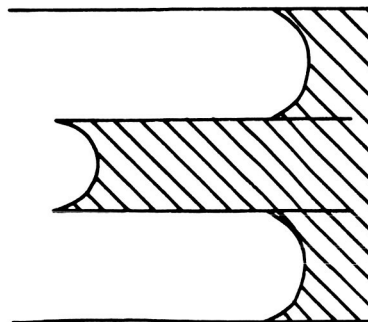
DECLASSIFIED  
CONFIDENTIAL



Tube radius is greater than one-half cylinder radius



Tube radius equals cylinder radius



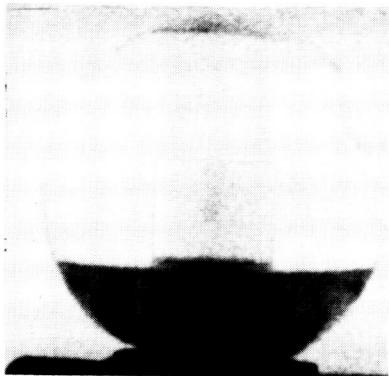
Tube radius is less than one-half the cylinder radius

Figure 3. - Effect of radius ratio on zero-gravity fluid configuration for cylinder with tube.

DECLASSIFIED  
CONFIDENTIAL

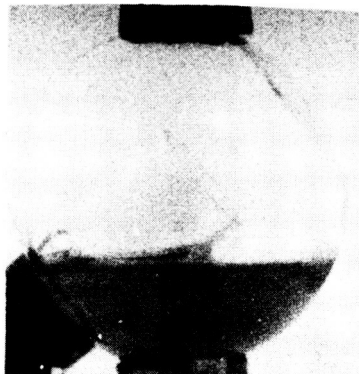
DECLASSIFIED  
CONFIDENTIAL

Control device  
in verticle position



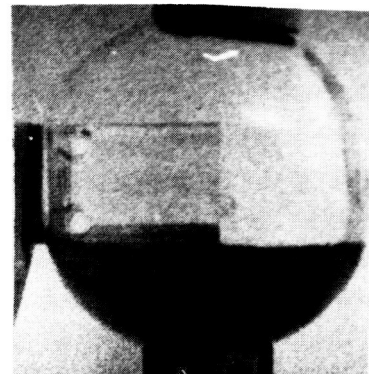
Time: 0 sec  
Frame: (a)

Control device  
at 45°

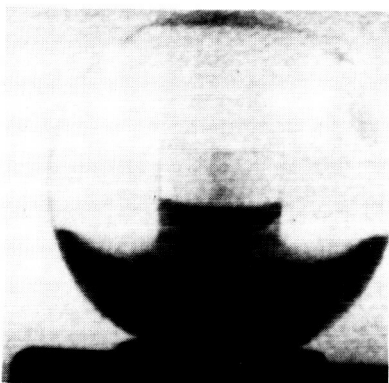


0 sec  
(d)

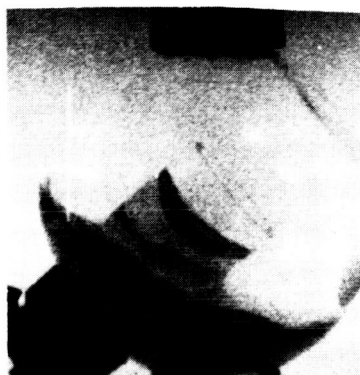
Control device  
at 90°



0 sec  
(g)



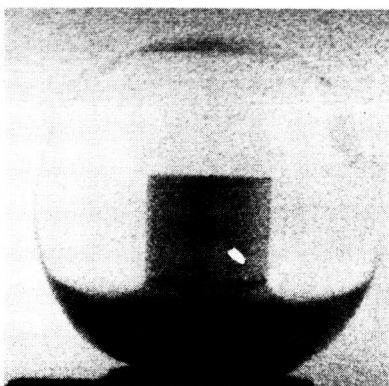
1/2 sec  
(b)



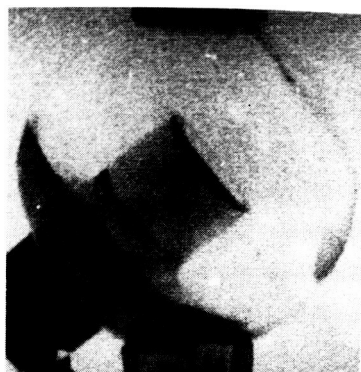
1/2 sec  
(e)



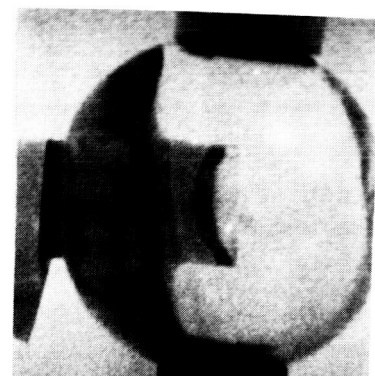
1/2 sec  
(h)



1-1/2 sec  
(c)



1-1/2 sec  
(f)



1-1/2 sec  
(i)

C-63773

Figure 4. - Capillary control device in drop-tower zero-gravity test with ethyl alcohol as the contained liquid.

DECLASSIFIED  
CONFIDENTIAL

CONFIDENTIAL  
DECLASSIFIED

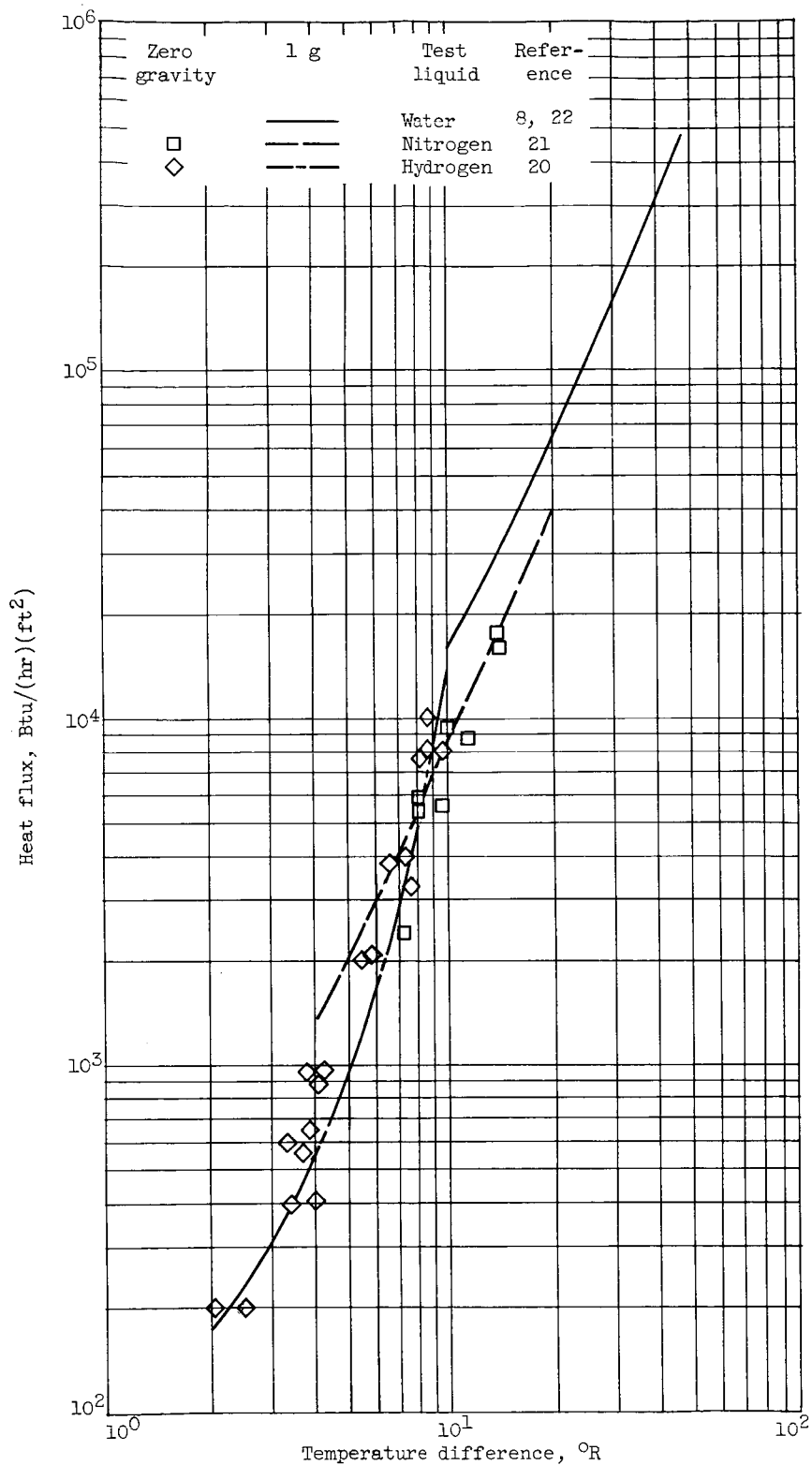


Figure 5. - Gravity effect on nucleate boiling heat transfer at atmospheric pressure.

CONFIDENTIAL  
DECLASSIFIED

DECLASSIFIED  
CONFIDENTIAL

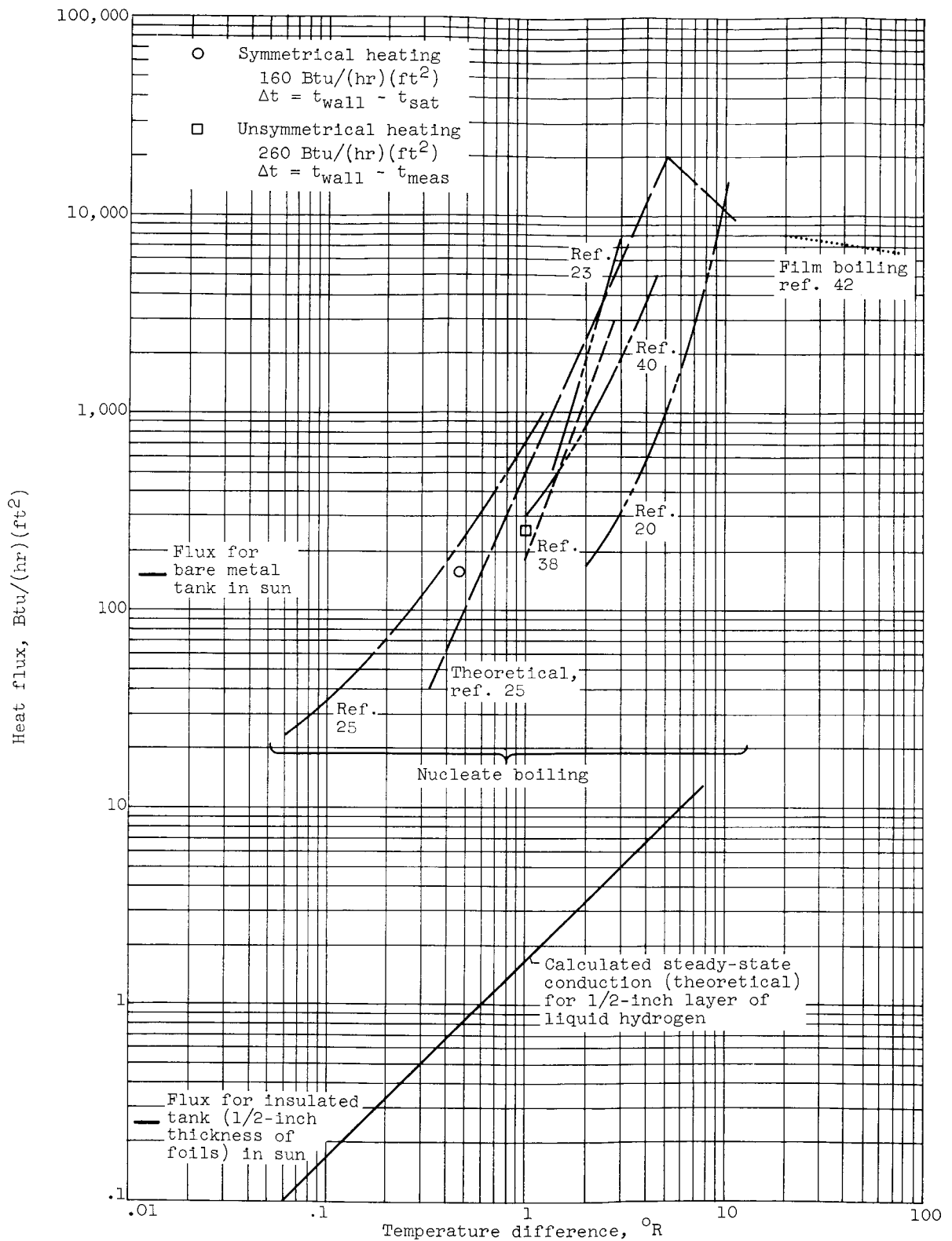
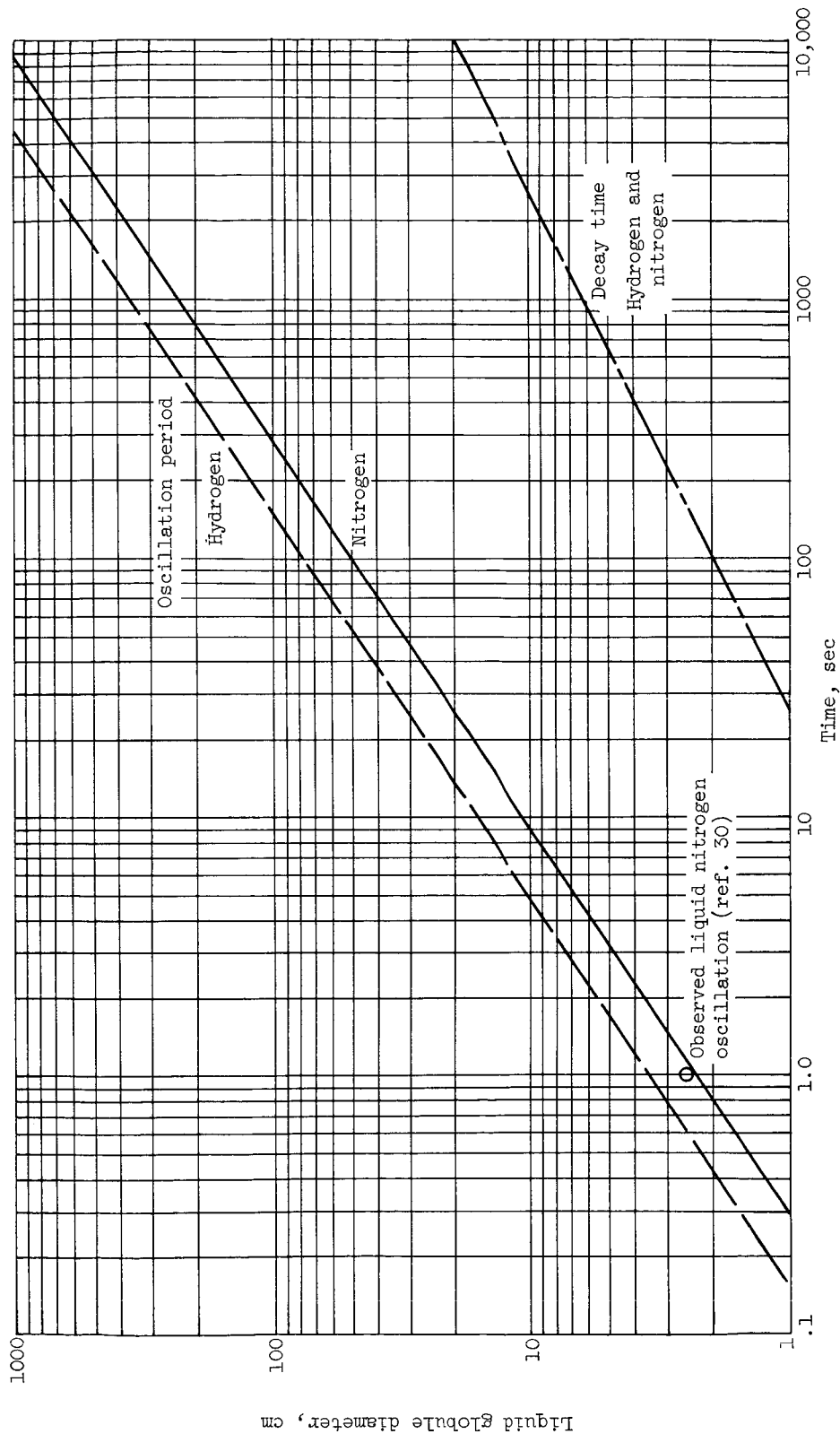


Figure 6. - Aerobee zero-gravity heat-transfer data for liquid hydrogen compared with reference data.

DECLASSIFIED  
CONFIDENTIAL

DECLASSIFIED  
CONFIDENTIAL

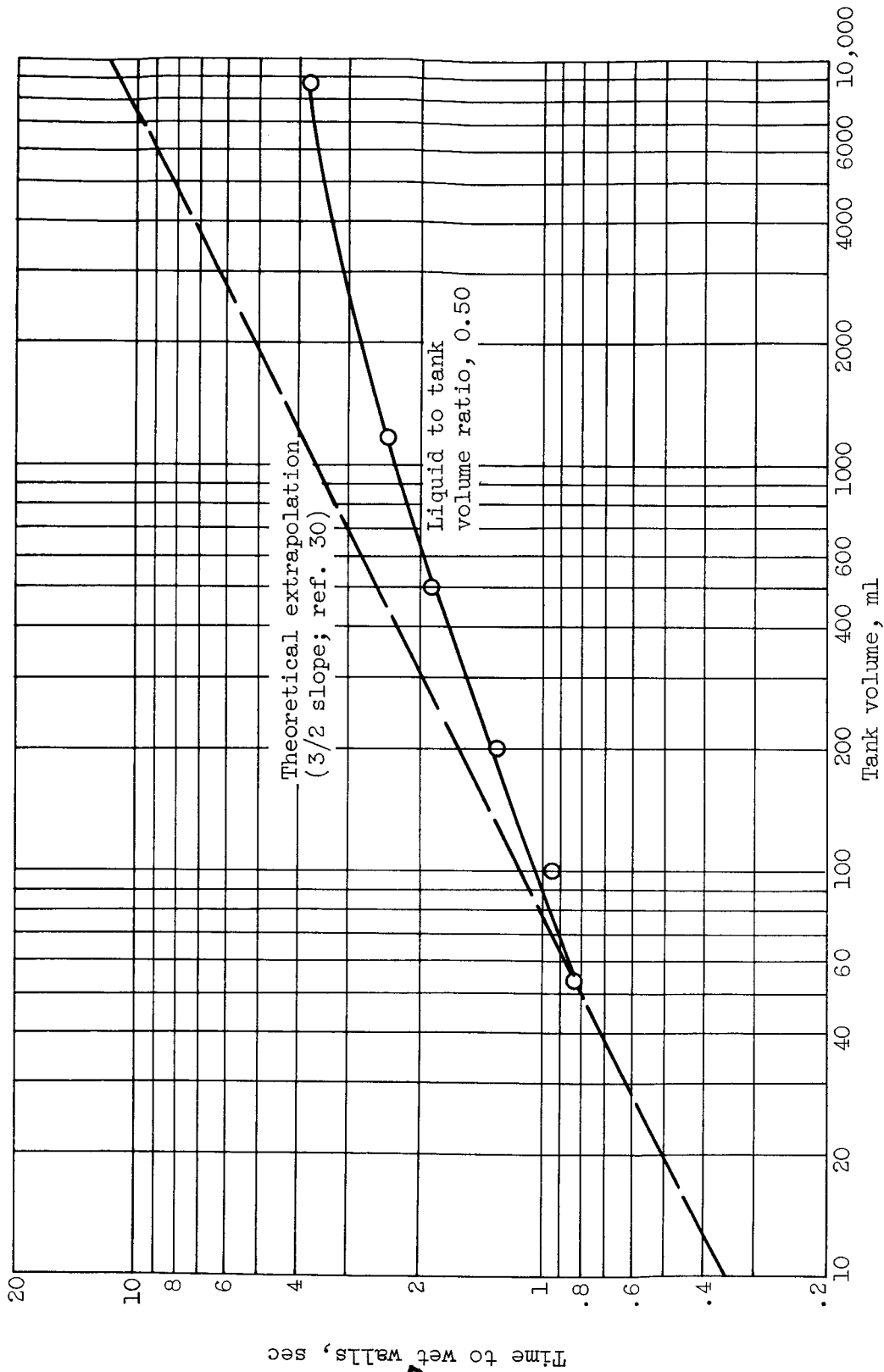


(a) Fundamental mode oscillation period and decay time  $\tau$  (times for original amplitude to decay by a factor  $1/e$ ).

Figure 7. - Study of scaling effects in zero-gravity environment.

DECLASSIFIED  
CONFIDENTIAL

DECLASSIFIED  
CONFIDENTIAL

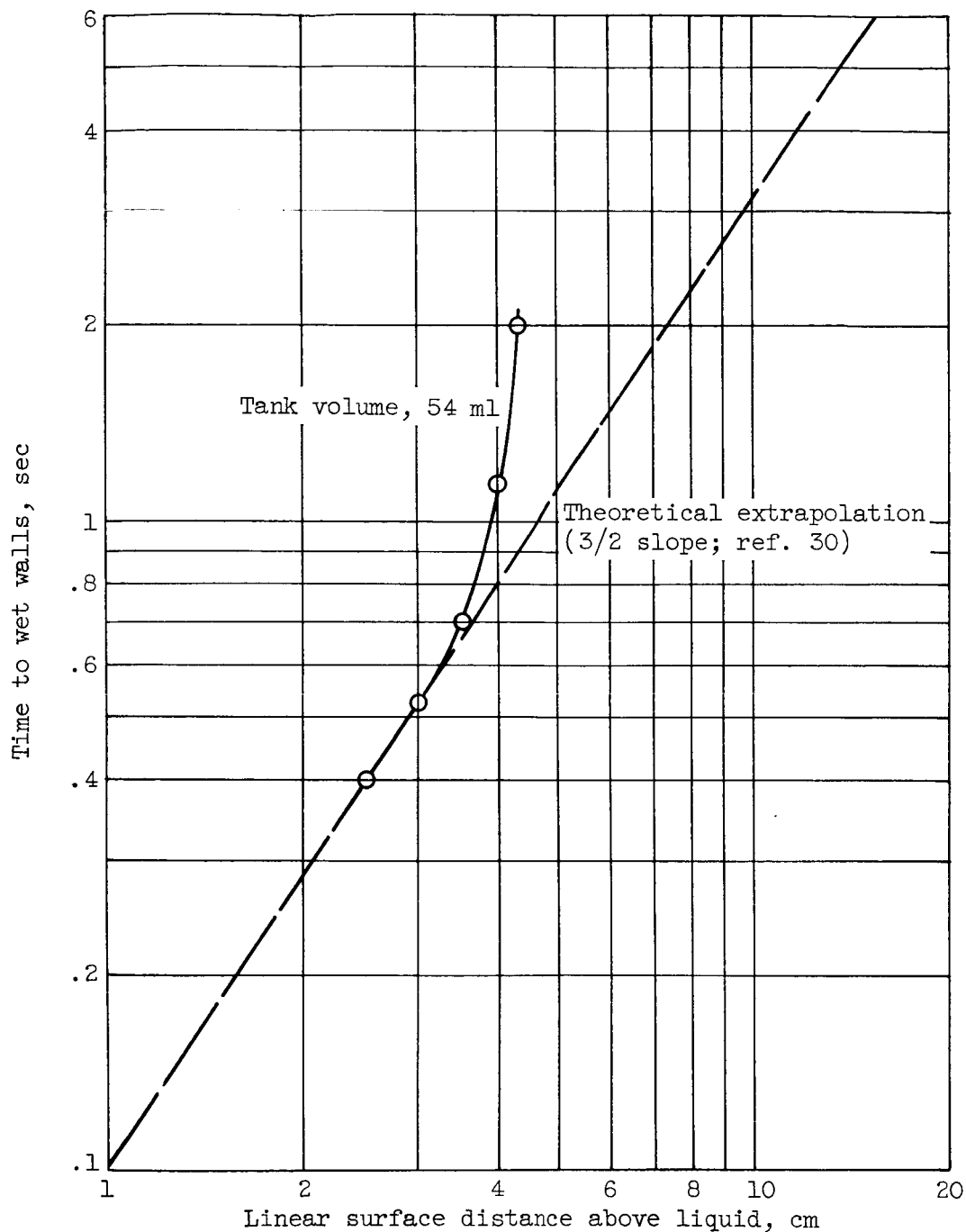


(b) Comparison with scaling theory on basis of liquid radius.

Figure 7. - Continued. Study of scaling effects in zero-gravity environment.

DECLASSIFIED  
CONFIDENTIAL

DECLASSIFIED  
CONFIDENTIAL



(c) Comparison with similarity law on the basis of distance to be wetted.

Figure 7. - Concluded. Study of scaling effects in zero-gravity environment.

DECLASSIFIED  
CONFIDENTIAL

DECLASSIFIED  
CONFIDENTIAL

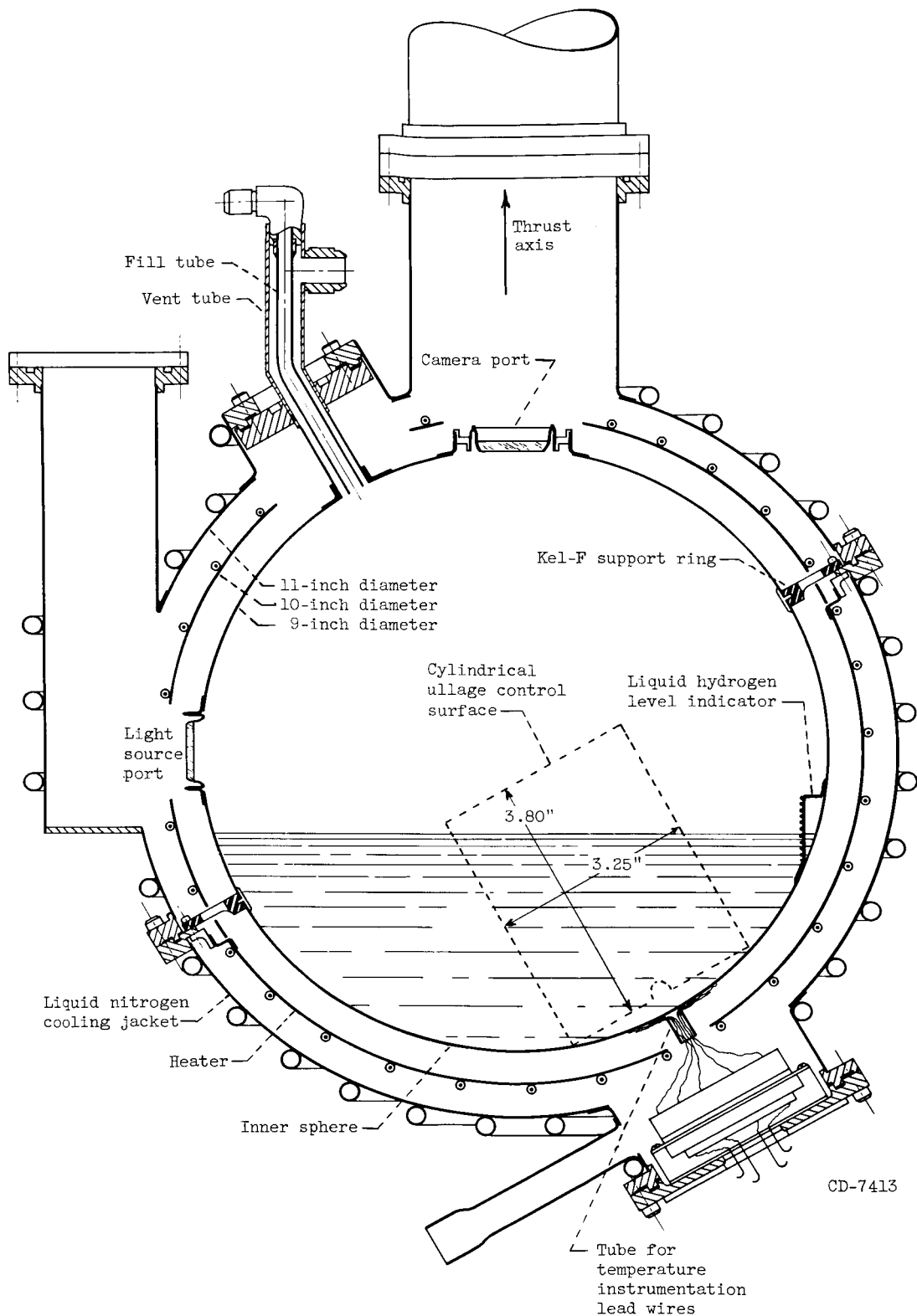


Figure 8. - Zero-gravity heat-transfer apparatus (Ref. 16).

DECLASSIFIED  
CONFIDENTIAL

DECLASSIFIED  
CONFIDENTIAL

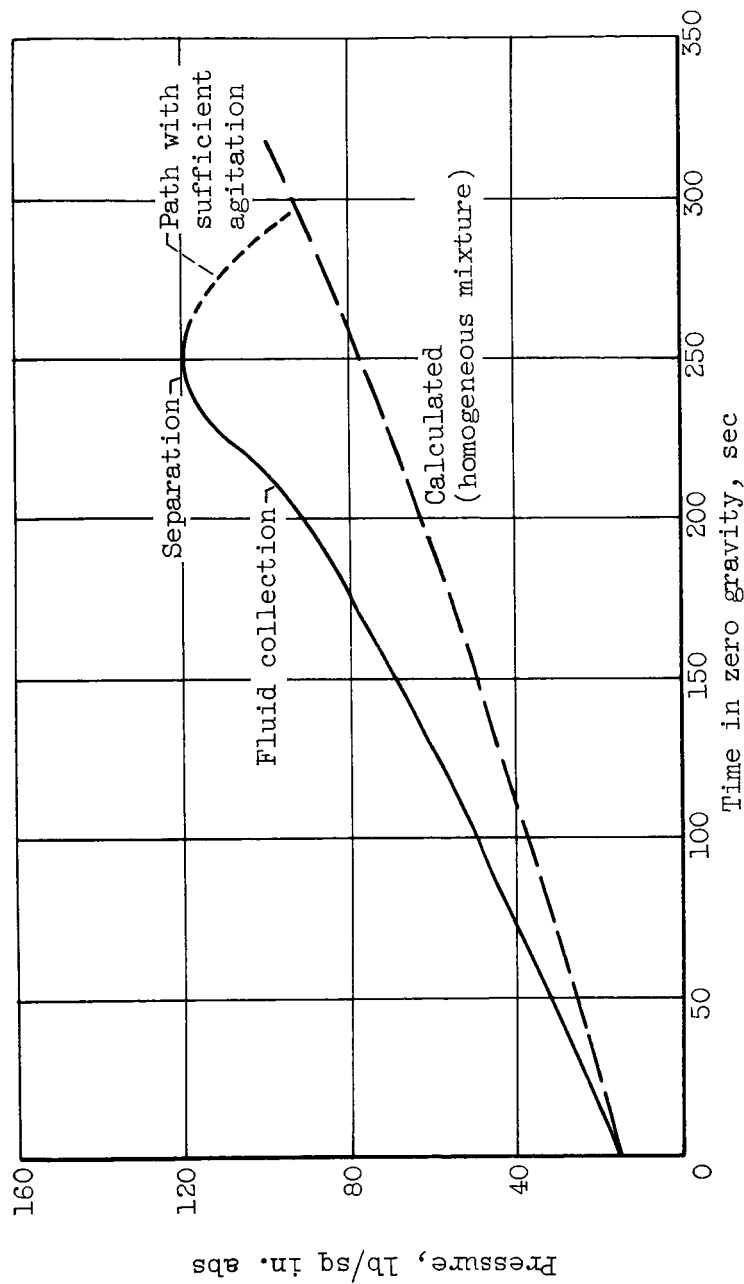


Figure 9. - Effect of zero gravity on tank pressure rise with heat addition. Uniform heating, 150 Btu per hour per foot squared.

DECLASSIFIED  
CONFIDENTIAL

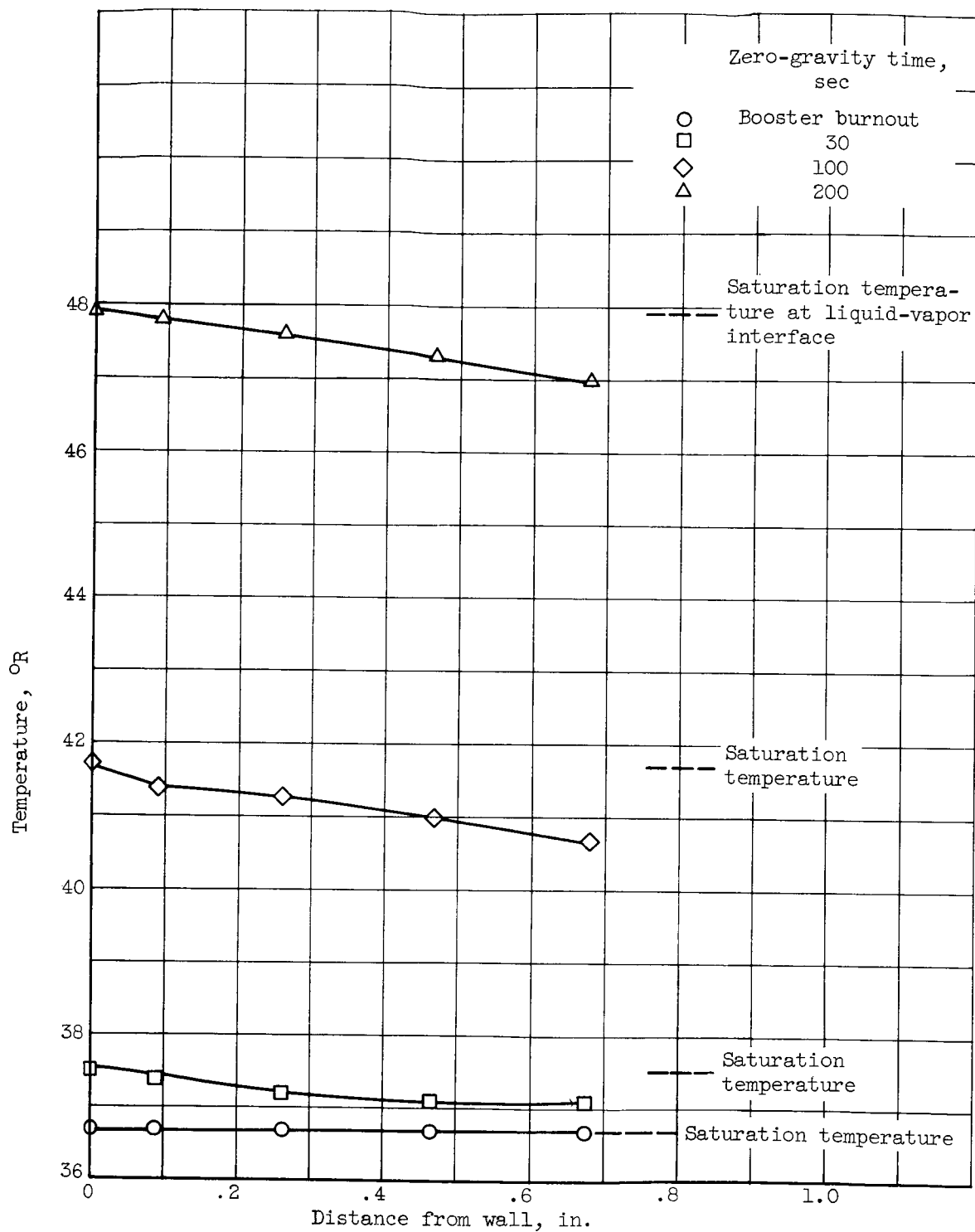


Figure 10. - Liquid hydrogen temperature gradient in 9-inch-diameter vessel 20 percent filled with liquid hydrogen. Unsymmetrical heating; thermocouple rake location shown in figure 8.

CONFIDENTIAL  
DECLASSIFIED

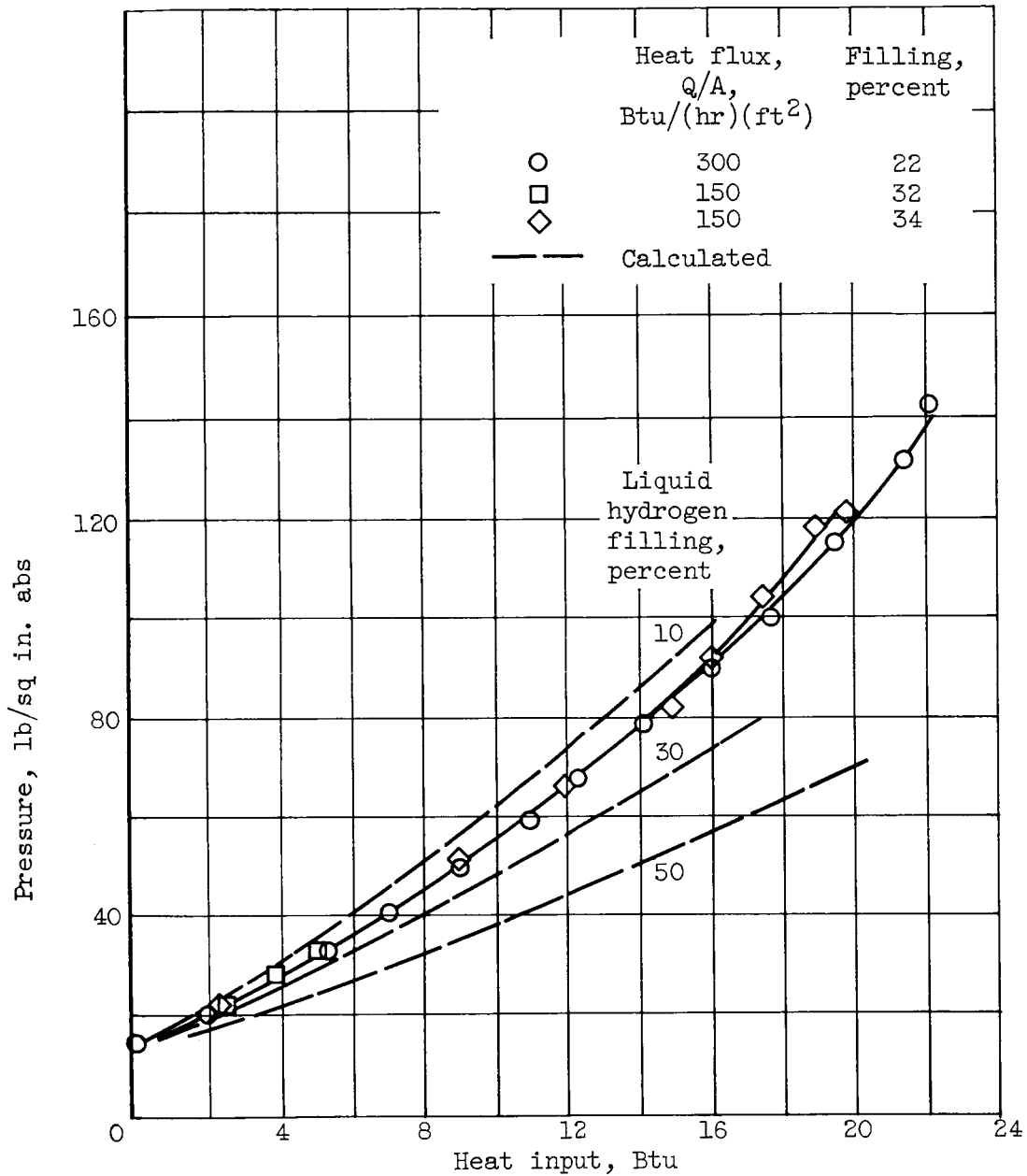


Figure 11. - Comparison of actual pressure rise with calculated pressure rise of a homogeneous mixture for zero-gravity experiment with 9-inch-diameter spherical vessel.

CONFIDENTIAL  
DECLASSIFIED

DECLASSIFIED  
CONFIDENTIAL

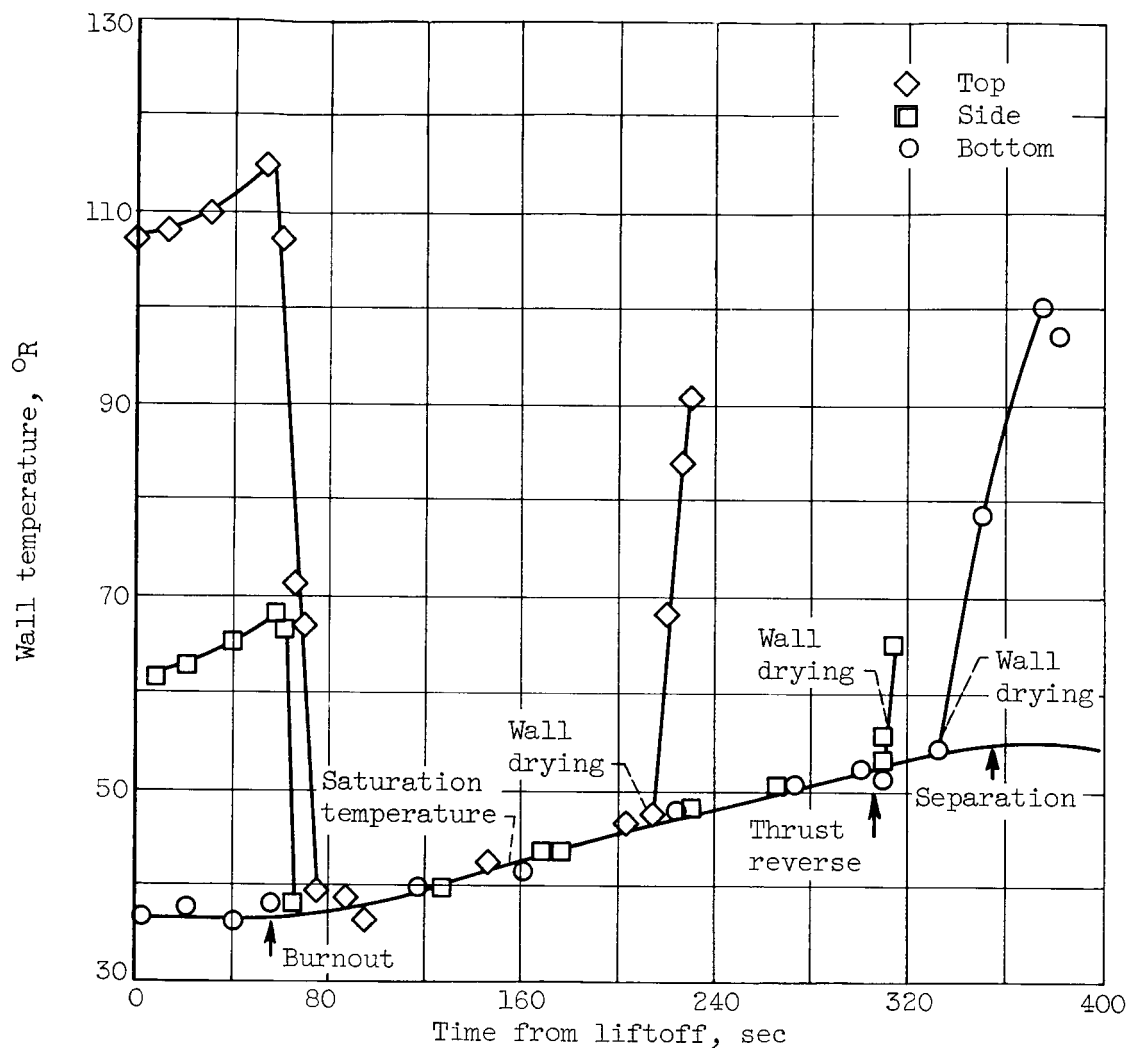
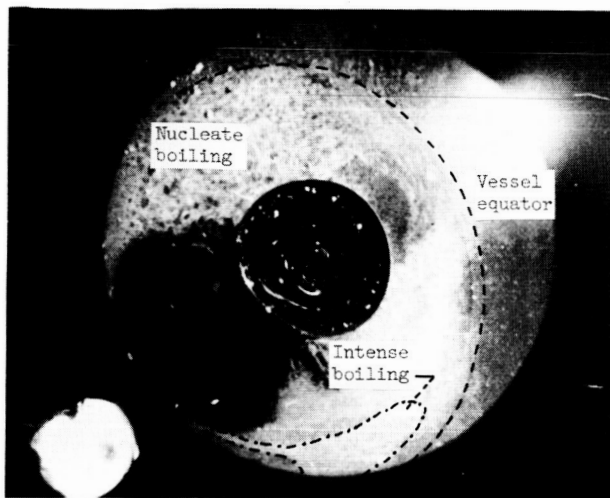


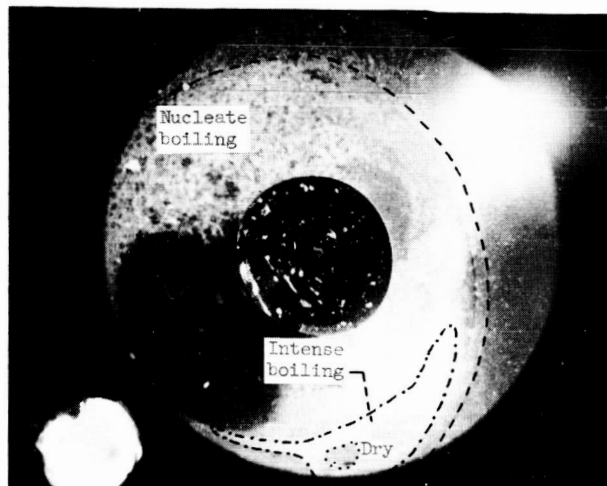
Figure 12. - Wall temperatures of 9-inch-diameter spherical vessel as a function of zero-gravity time. Uniform heat flux about 150 Btu per hour per foot squared (data from Aerobee Rocket test).

DECLASSIFIED  
CONFIDENTIAL

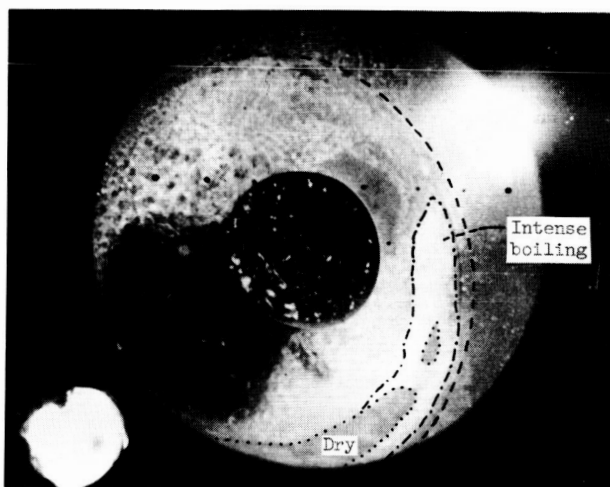
DECLASSIFIED  
CONFIDENTIAL



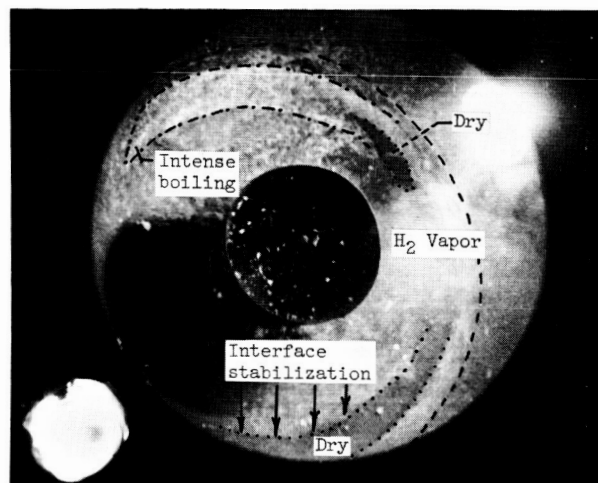
(a) White spot indicates transfer from nucleate to intense boiling. Zero-gravity time, 206 seconds.



(b) Black spot indicates start of wall drying. Zero-gravity time, 209 seconds.



(c) Wall-drying and boiling areas spread. Liquid-vapor interface at wall is stabilized. Zero-gravity time, 223 seconds.



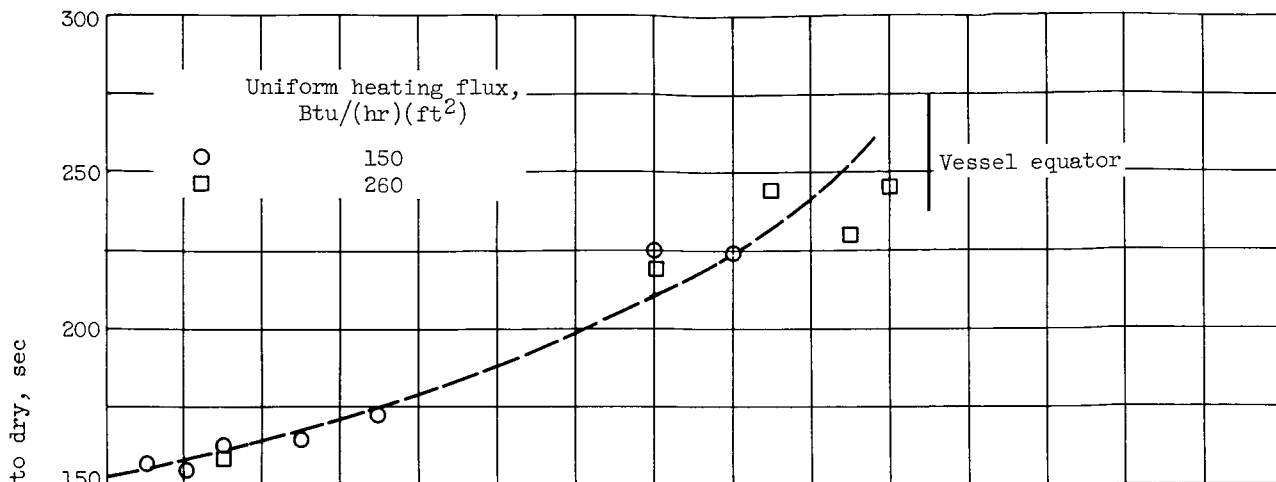
(d) Hydrogen vapor clouds and large dry zone form. Zero-gravity time, 253 seconds.

C-63774

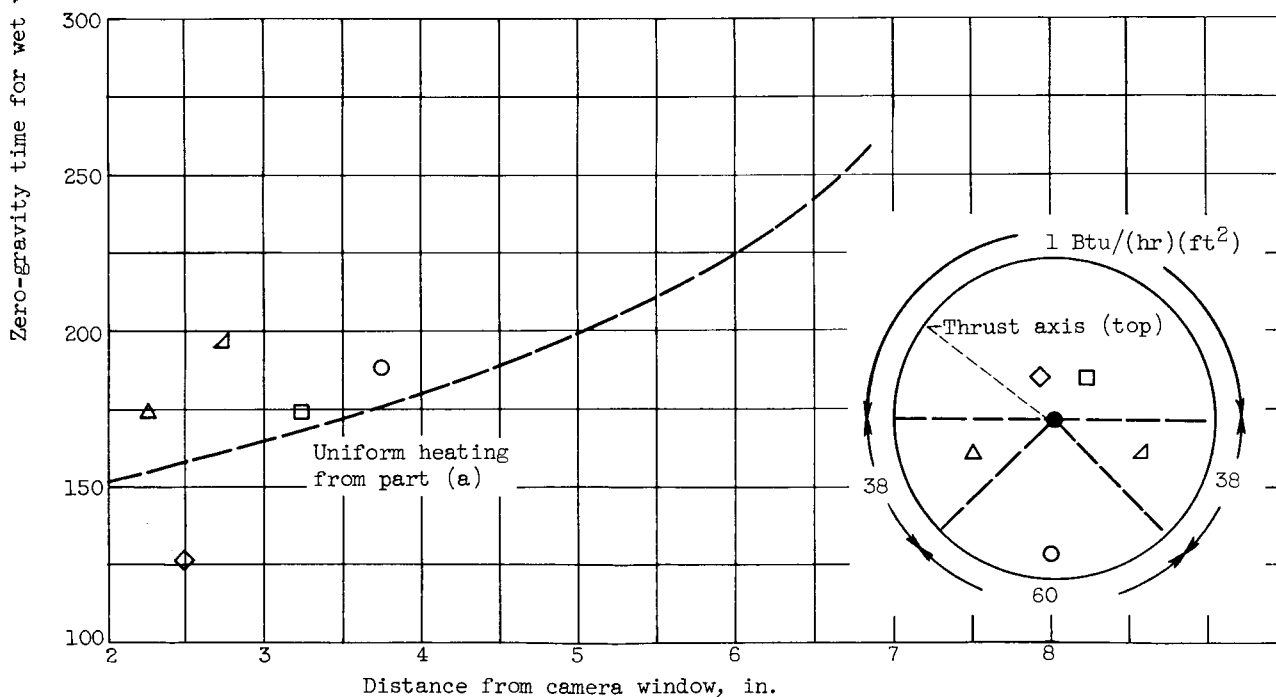
Figure 13. - Evaluation of wall-drying process for liquid hydrogen in a 9-inch-diameter spherical container in zero gravity. (Heat flux to left of equator  $250 \text{ Btu}/(\text{hr})(\text{ft}^2)$ , to right of equator  $\sim 1 \text{ Btu}/(\text{hr})(\text{ft}^2)$ .)

DECLASSIFIED  
CONFIDENTIAL

DECLASSIFIED  
CONFIDENTIAL



(a) Uniform heating.



(b) Nonuniform heating.

Figure 14. - Zero-gravity time for inception of wall drying in a hydrogen-liquid-wetted 9-inch-diameter spherical vessel.

DECLASSIFIED  
CONFIDENTIAL

DECLASSIFIED  
CONFIDENTIAL

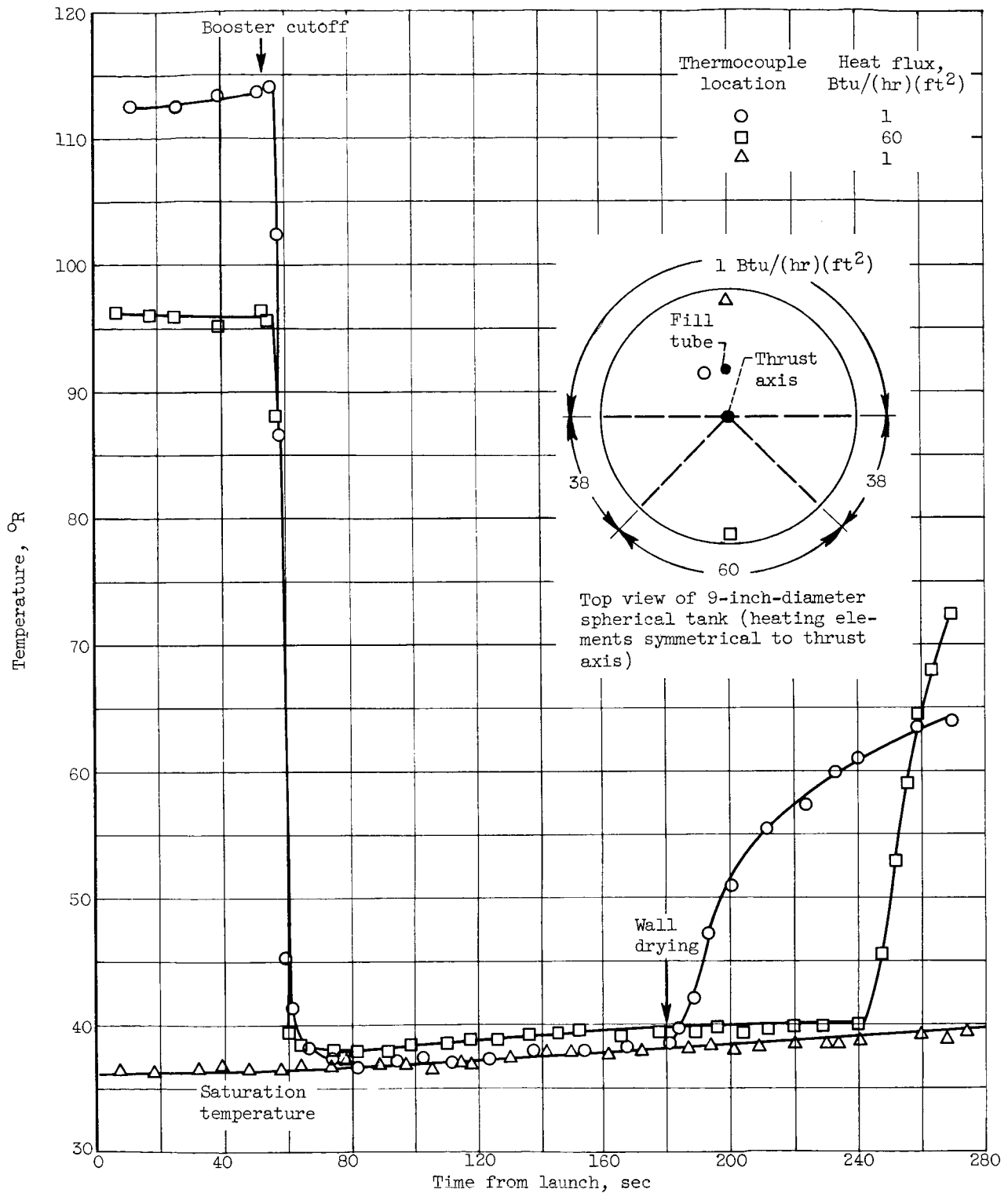


Figure 15. - Wall temperatures of closed spherical vessel in zero gravity with un-symmetrical heating.

DECLASSIFIED  
CONFIDENTIAL

DECLASSIFIED  
CONFIDENTIAL

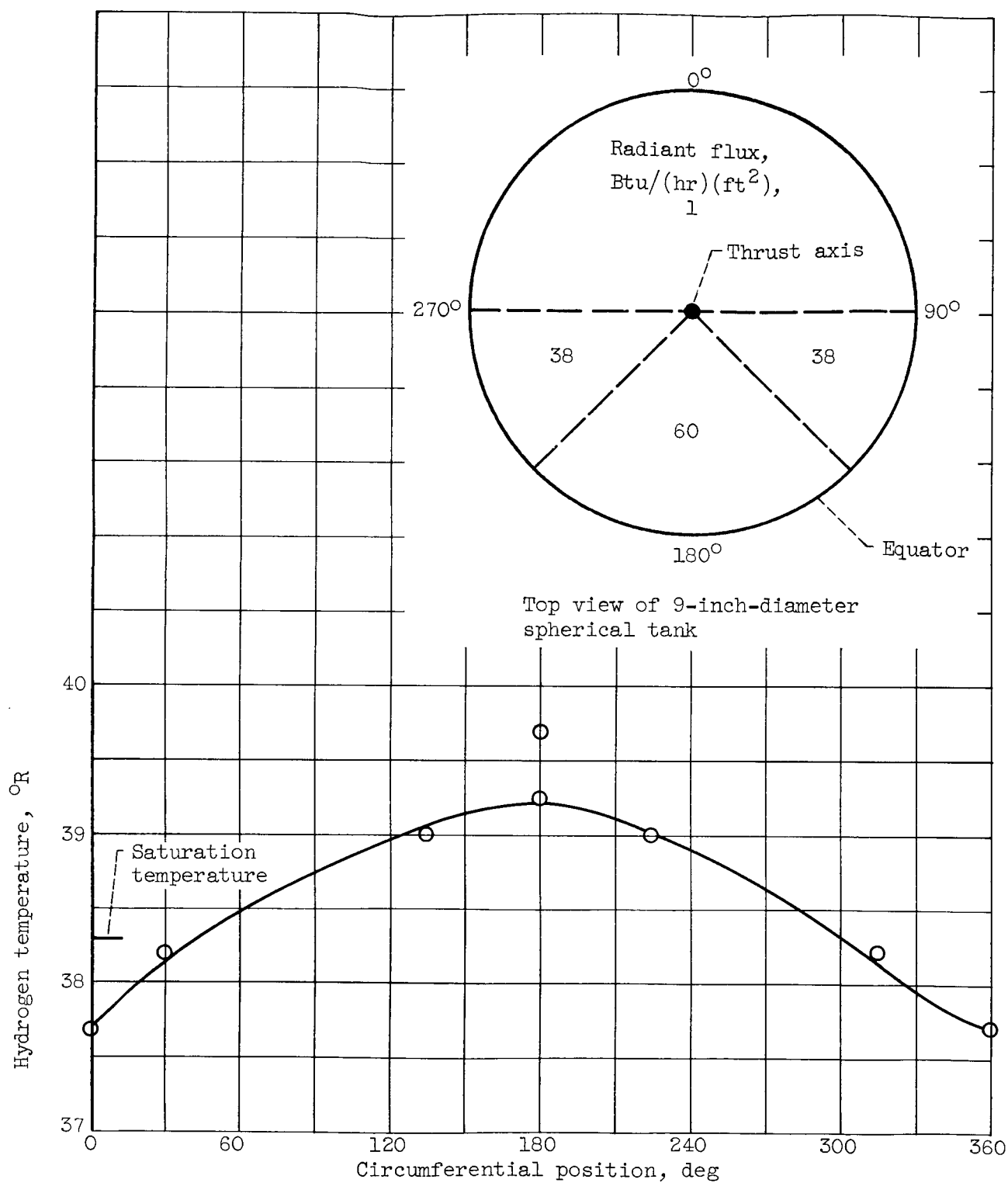


Figure 16. - Temperature distribution around equator of unsymmetrically heated sphere at 160 seconds after liftoff.

DECLASSIFIED  
CONFIDENTIAL

DECLASSIFIED  
CONFIDENTIAL

Inception of wall drying

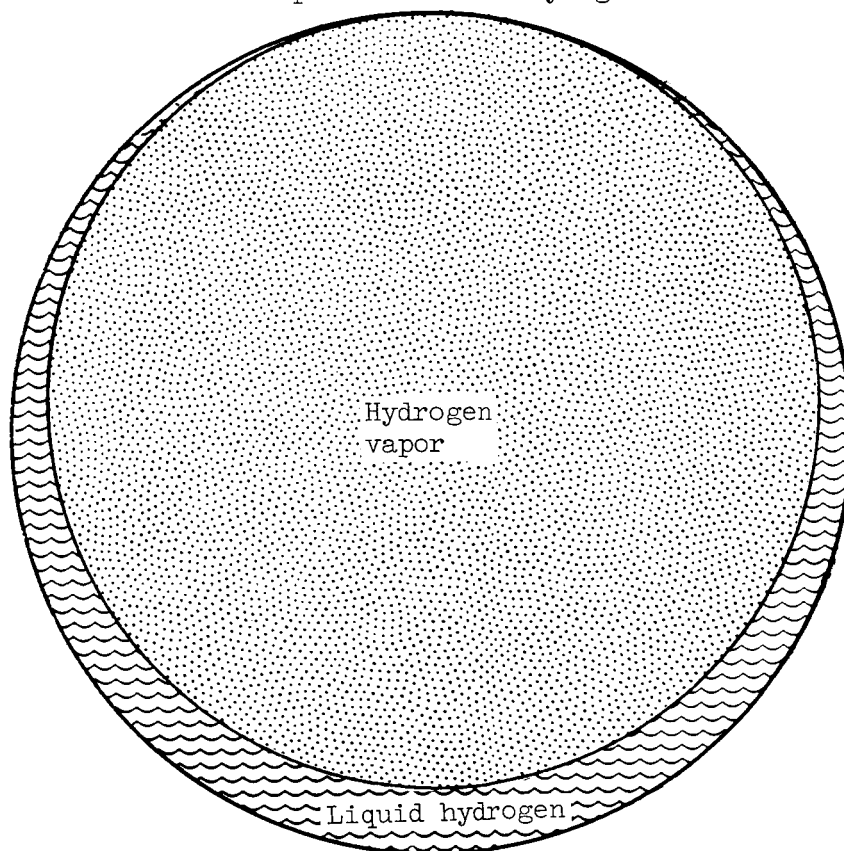


Figure 17. - Aerobee 9-inch-diameter Dewar tank  
30-percent filled with liquid hydrogen. Spherical  
vapor ullage tangent to top of vessel.

DECLASSIFIED  
CONFIDENTIAL

DECLASSIFIED  
CONFIDENTIAL

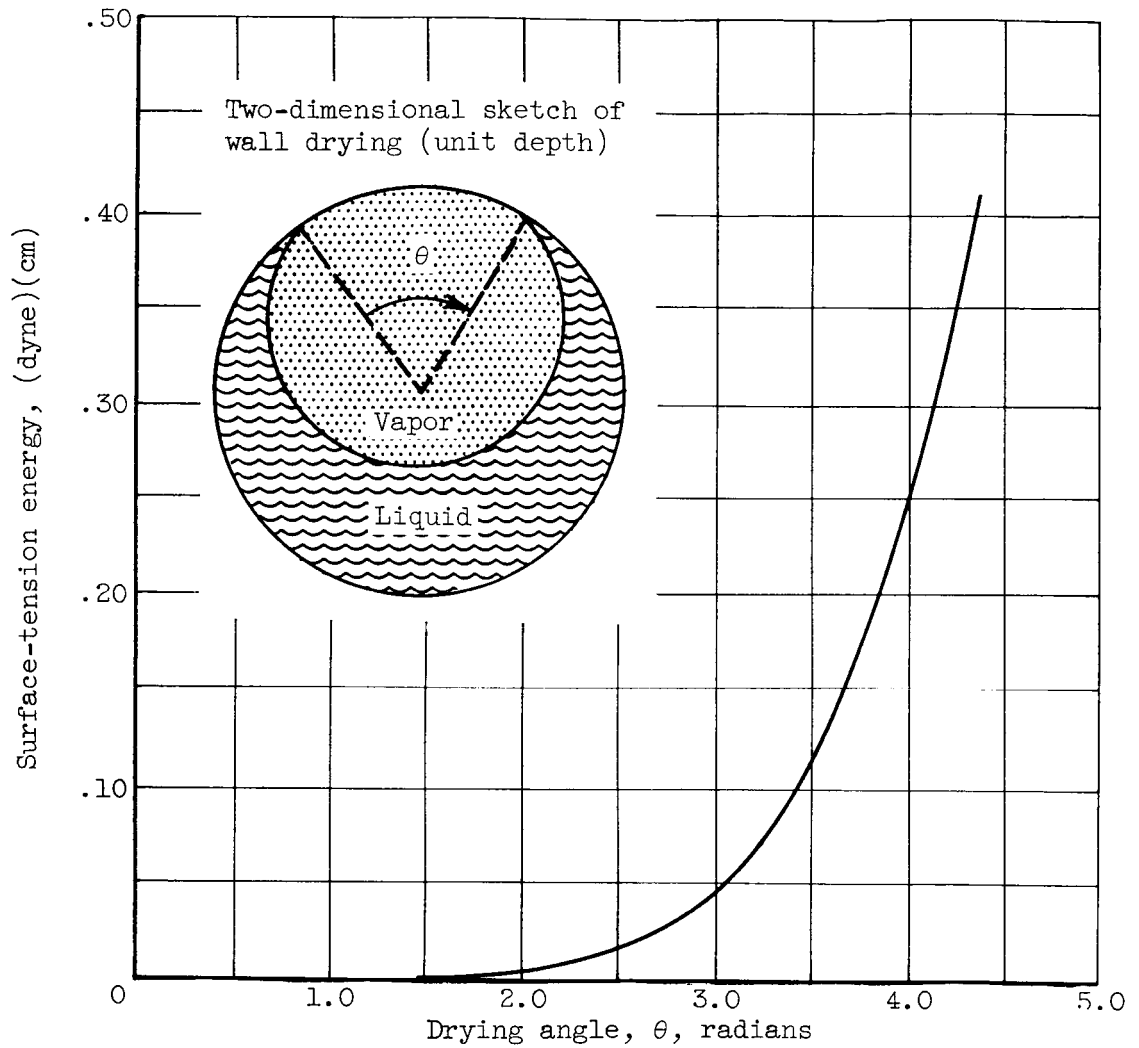
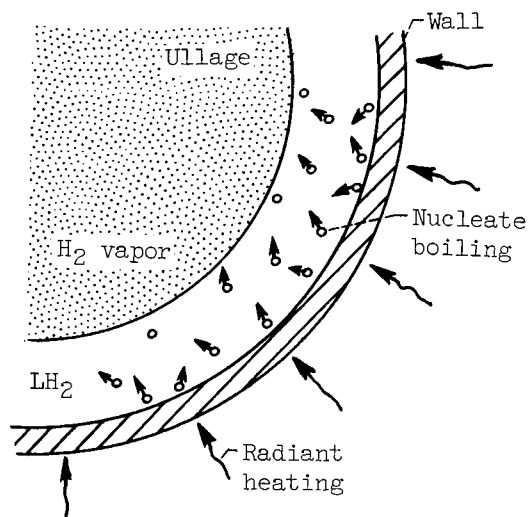


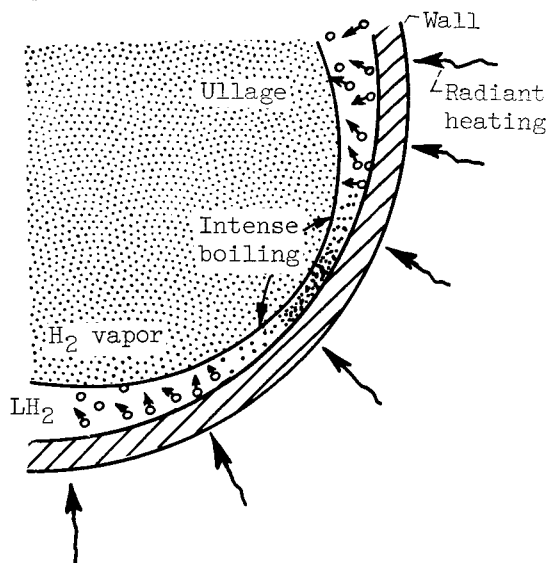
Figure 18. - Calculated variation of surface-tension energy with wall-drying angle in zero gravity.

DECLASSIFIED  
CONFIDENTIAL

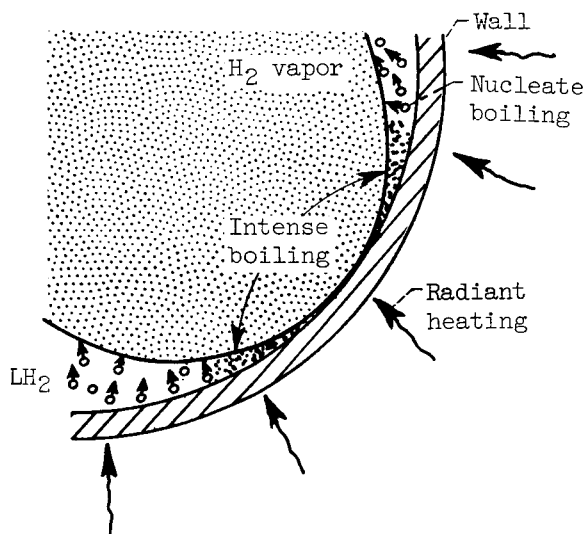
DECLASSIFIED  
CONFIDENTIAL



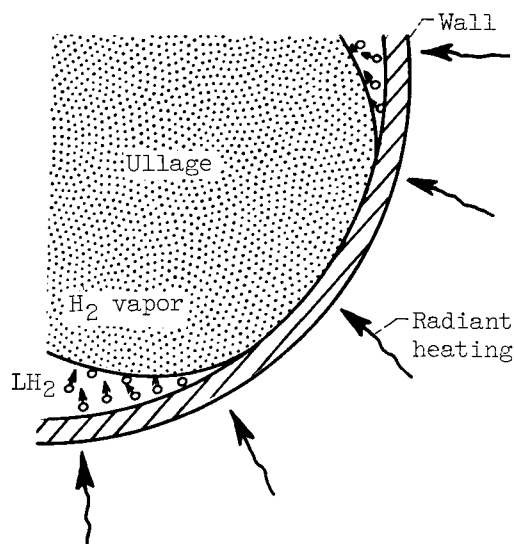
(a) Sphere with liquid hydrogen and radiant heat input with nucleate boiling at wall. Condensation in liquid and at liquid-vapor interface.



(b) Random movement of ullage toward vessel wall thins liquid layer and results in intense boiling (more vapor entrainment) at closest point of ullage to vessel wall.



(c) Low heat capacity in thin liquid film at intense-boiling region forces evaporation at a rate faster than surface-tension forces can circulate liquid, which results in a "dry" spot with a local rise in wall temperature.



(d) Large dry area and increased surface-tension forces increase liquid circulation to eliminate intense boiling at wet to dry wall interface. The drying process has thus been stabilized (see fig. 13(c) and (d)).

Figure 19. - Sequence of wall-drying process in zero gravity.

DECLASSIFIED  
CONFIDENTIAL

DECLASSIFIED  
CONFIDENTIAL

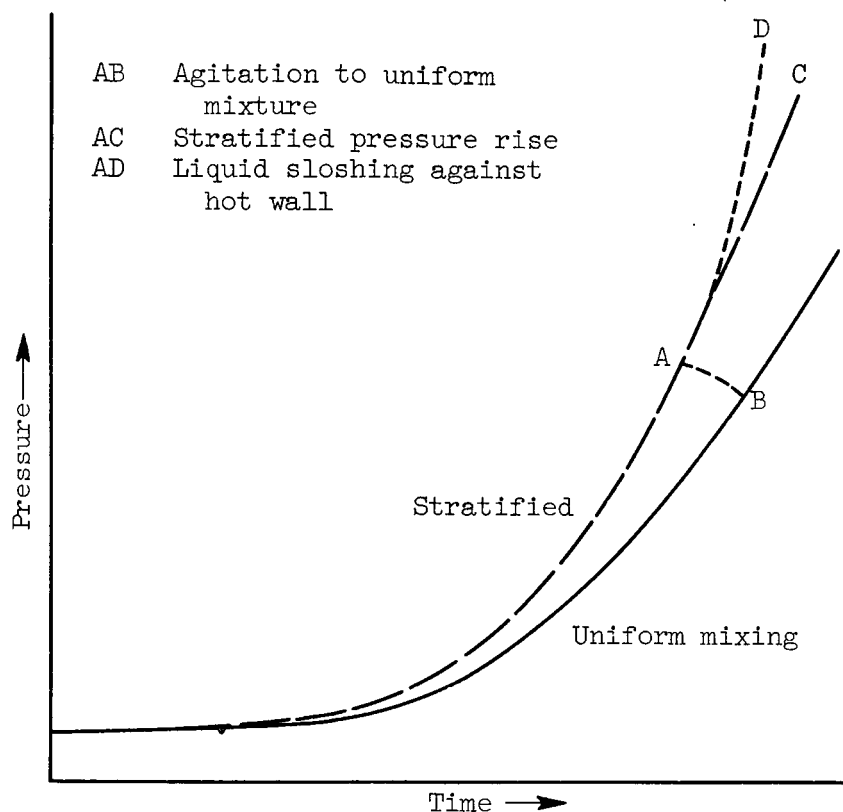


Figure 20. - Pressure rise in a closed vessel showing possible paths with agitation, heat addition, and sloshing.

DECLASSIFIED  
CONFIDENTIAL

DECLASSIFIED  
CONFIDENTIAL

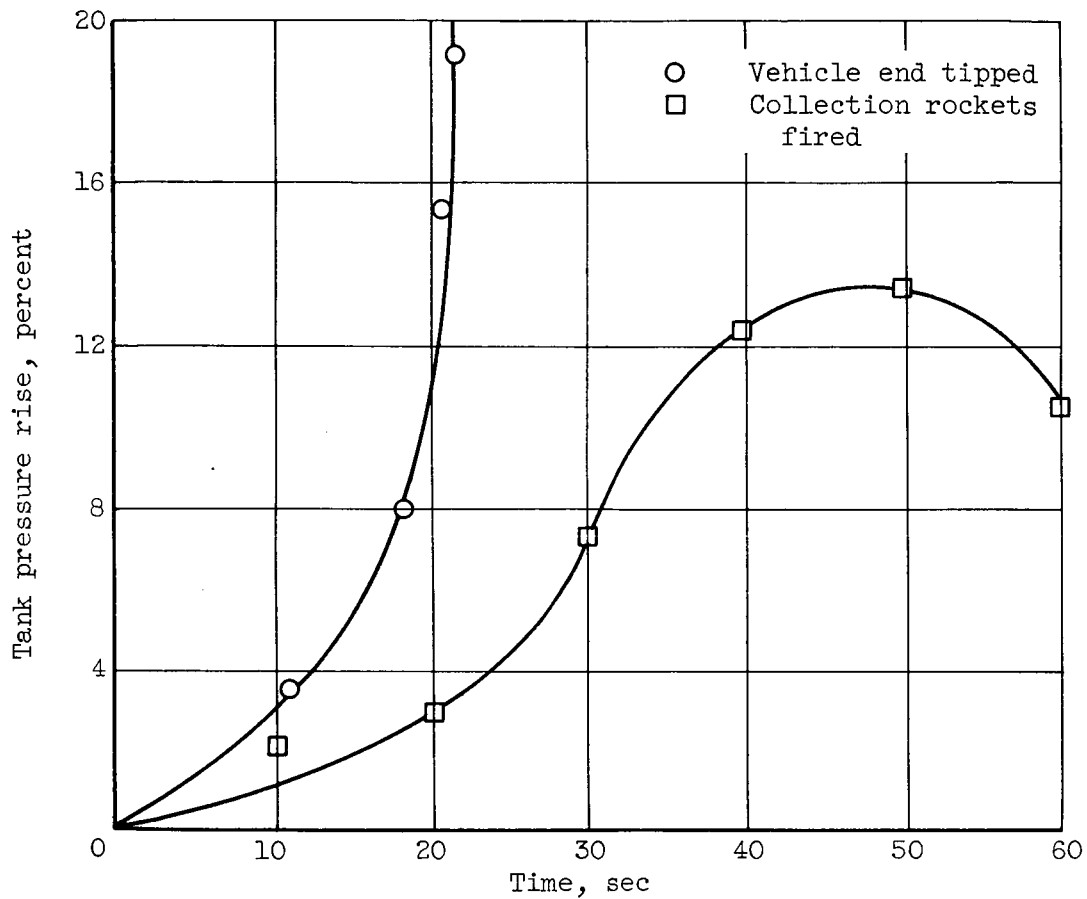


Figure 21. - Pressure rise resulting from sloshing against dry tank wall.

DECLASSIFIED  
CONFIDENTIAL

DECLASSIFIED  
CONFIDENTIAL

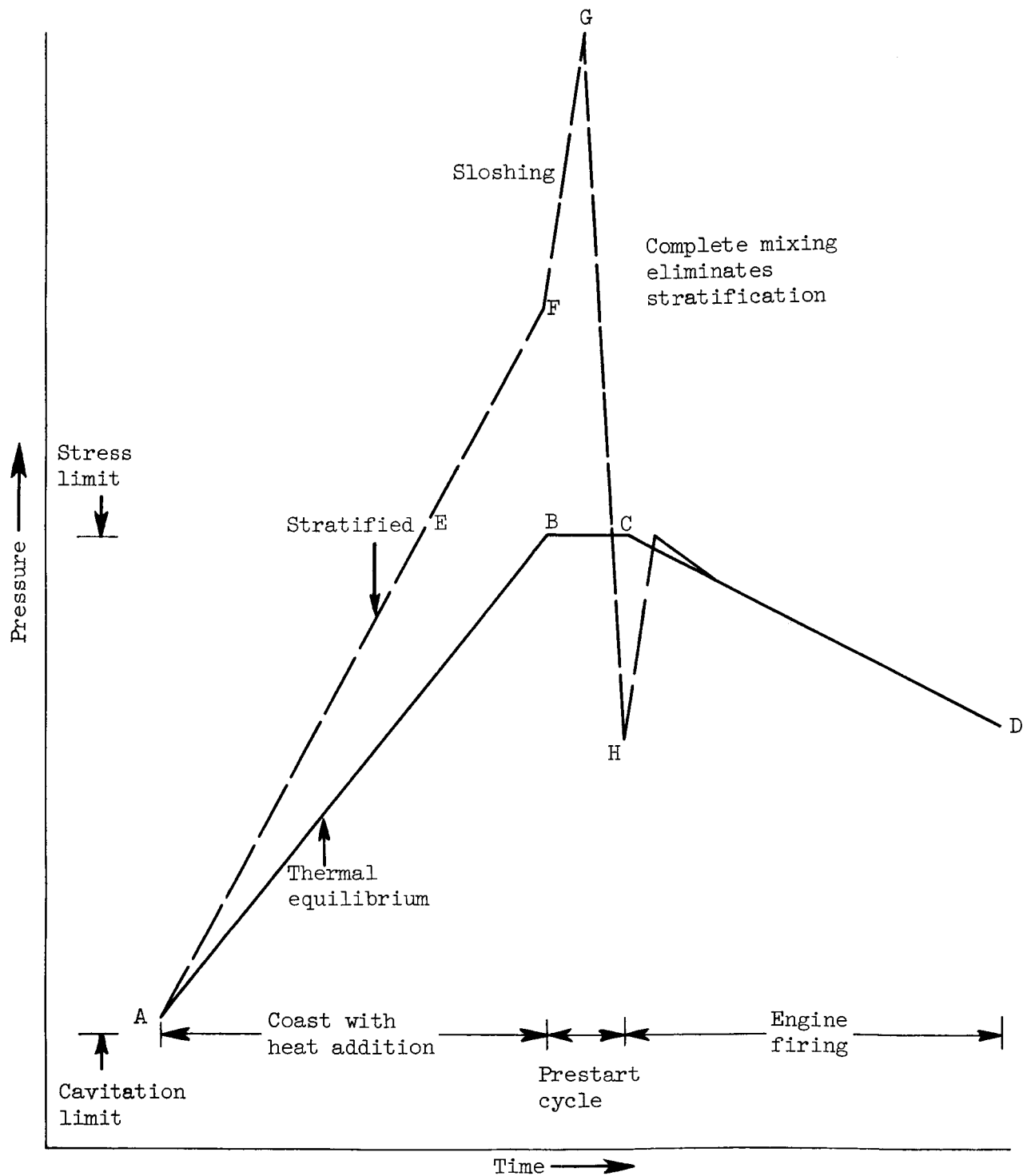
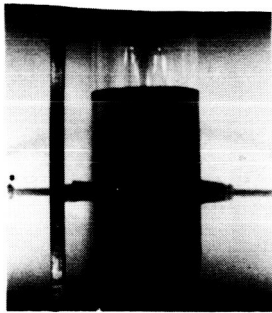


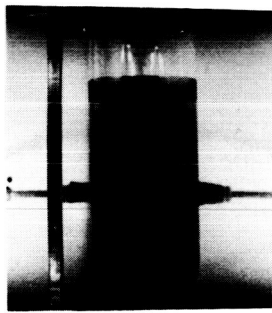
Figure 22. - Possible significance of some zero-gravity effects on liquid hydrogen storage system.

DECLASSIFIED  
CONFIDENTIAL

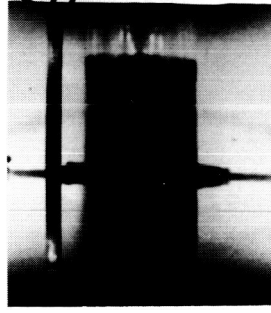
DECLASSIFIED  
CONFIDENTIAL



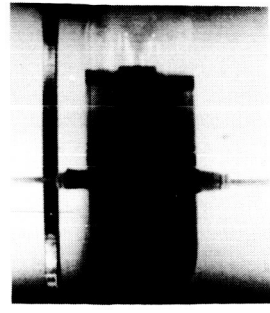
(a)



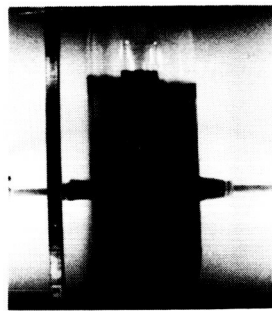
(b)



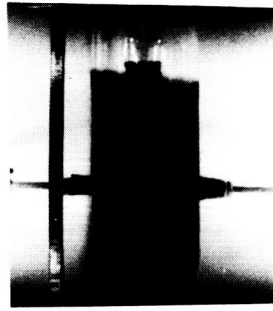
(c)



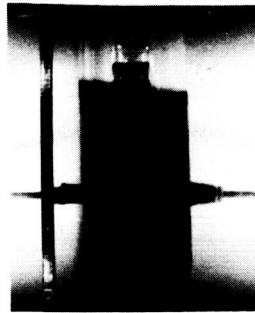
(d)



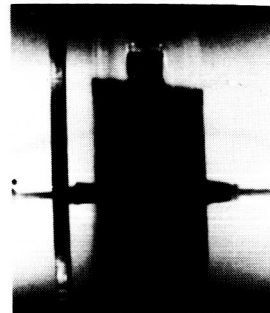
(e)



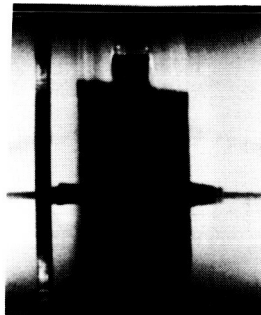
(f)



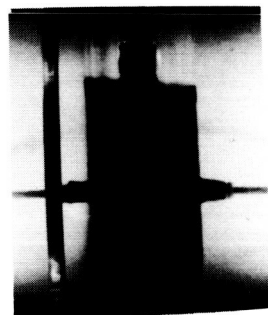
(g)



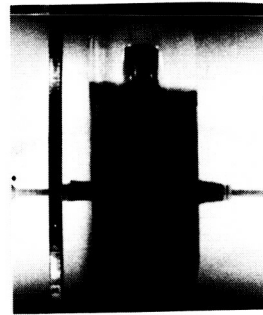
(h)



(i)



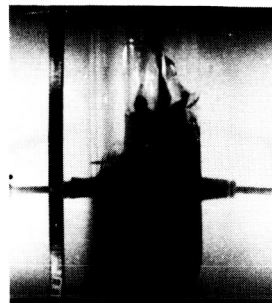
(j)



(k)



(l)



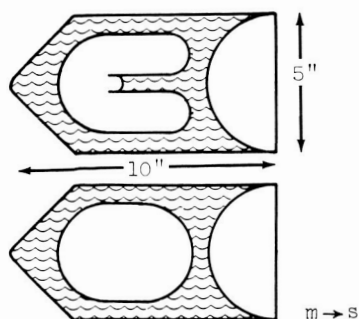
(m)

C-63775

Figure 23. - Alcohol contained in a 5-inch-diameter cylindrical tank with a capillary control tube in zero-gravity free-fall experiment. Exposure interval about 0.2 second.

DECLASSIFIED  
CONFIDENTIAL

DECLASSIFIED  
CONFIDENTIAL



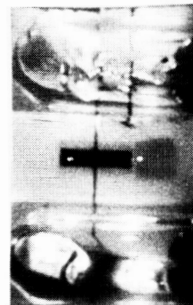
Configuration sketch showing completely wetted walls



(a)



(b)



(c)



(d)



(e)



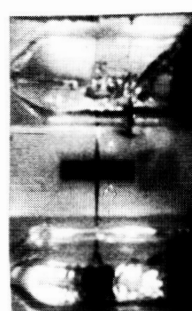
(f)



(g)



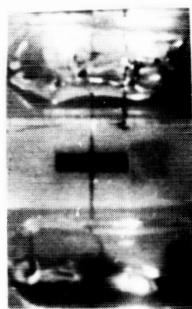
(h)



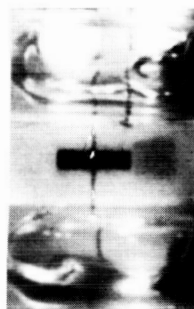
(i)



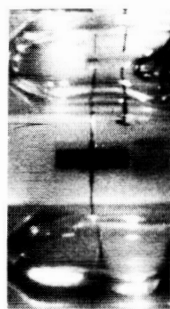
(j)



(k)



(l)



(m)



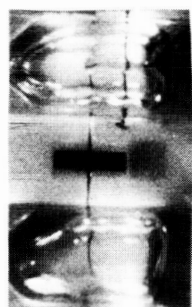
(n)



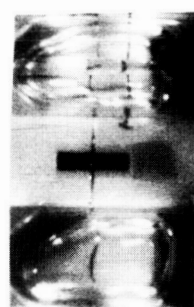
(o)



(p)



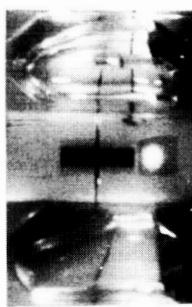
(q)



(r)



(s)



(t)

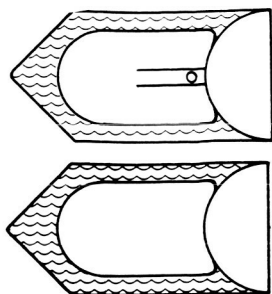
C-63776

a - b 2-1/2 g pullup  
c - 1 decreasing gravity  
j - s near zero gravity  
t start pullout maneuver

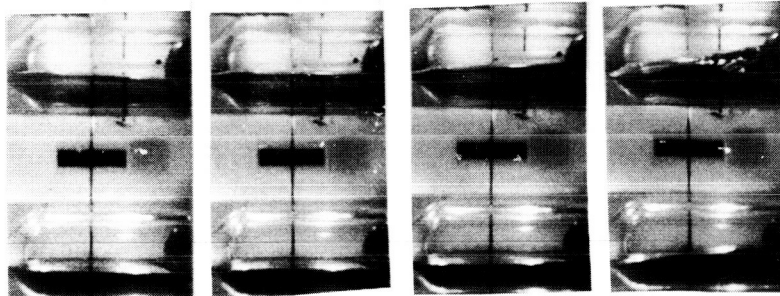
Figure 24. - Alcohol in a 5-inch-diameter 50-percent filled cylindrical tank with and without capillary control tube; filmed at one second intervals during zero-gravity airplane maneuver (Ref. 35).

DECLASSIFIED  
CONFIDENTIAL

DECLASSIFIED  
CONFIDENTIAL



Configuration sketch showing partially wetted walls

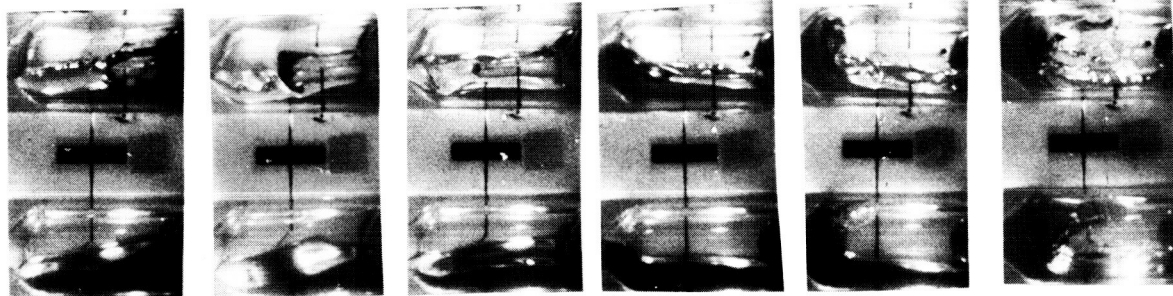


(a)

(b)

(c)

(d)



(e)

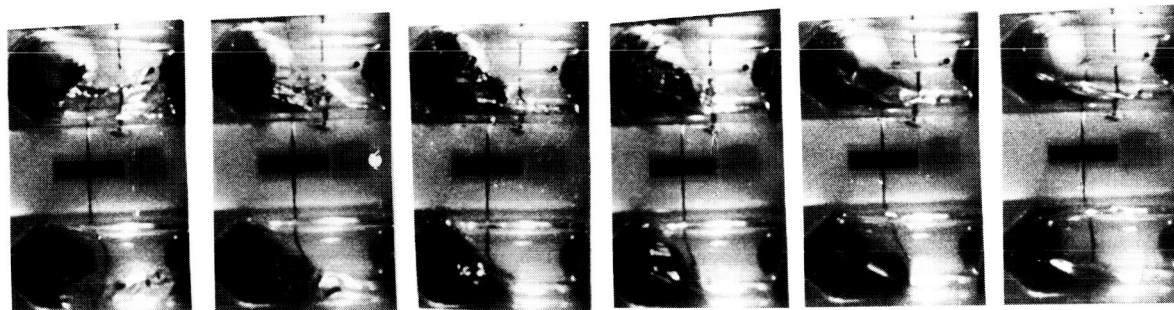
(f) Release

(g)

(h)

(i)

(j)



(k)

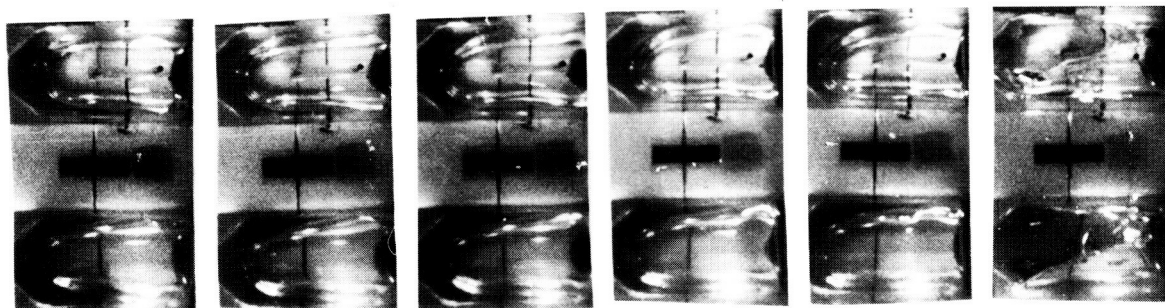
(l)

(m)

(n)

(o)

(p)



(q)

(r)

(s)

(t)

(u)

(v)

a - d 2-1/2 g pullup  
e - m decreasing gravity  
n - u near zero gravity  
v start pullout maneuver

C-63777

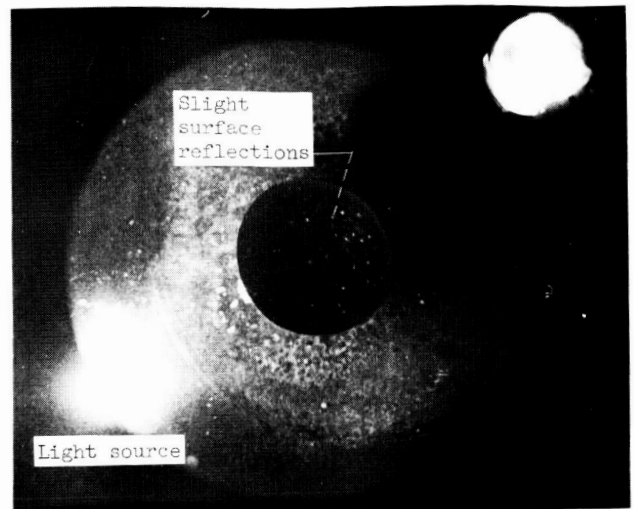
Figure 25. - Weightlessness behavior of alcohol contained in a 5-inch-model 50-percent-filled cylindrical tank with and without capillary control tube; filmed at one-second intervals during zero-gravity airplane maneuver (Ref. 35).

DECLASSIFIED  
CONFIDENTIAL

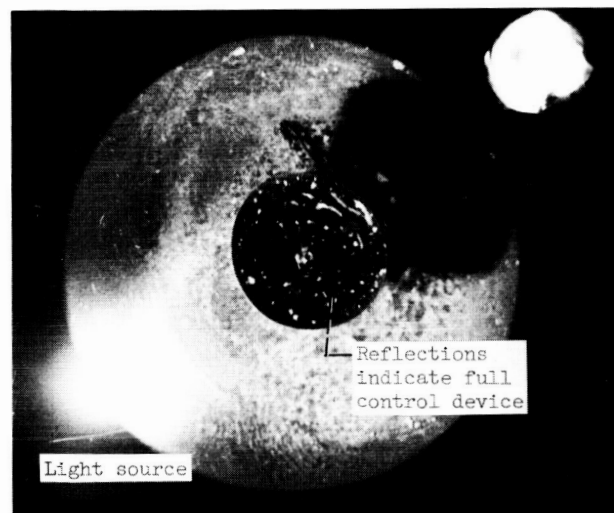
DECLASSIFIED  
CONFIDENTIAL



(a) No light reflection in control device indicates it is nearly empty of liquid hydrogen at start of zero-gravity period.



(b) Surface reflection at right in control device indicates it is partly filled with liquid hydrogen after 48 seconds of zero gravity.



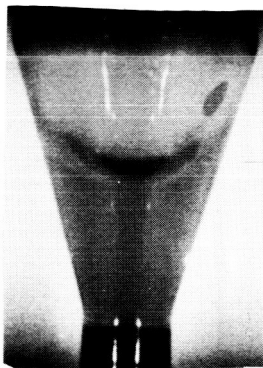
C-63778

(c) Surface reflection over entire area in control device indicates it is nearly filled, after 194 seconds of zero gravity.

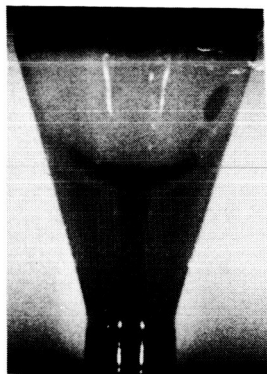
Figure 26. - Top view through camera lens of 9-inch-diameter sphere with 3-1/4-inch-diameter by 3.8-inch cylindrical control device located about 30° from bottom of sphere. Filled 20 percent with liquid hydrogen (see fig. 8.).

DECLASSIFIED  
CONFIDENTIAL

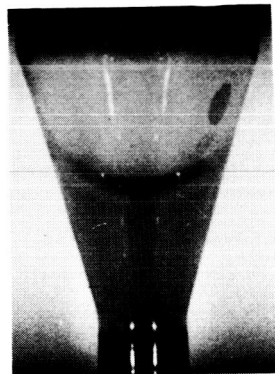
DECLASSIFIED  
CONFIDENTIAL



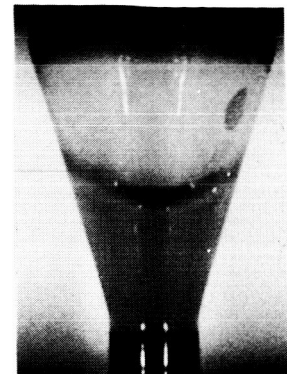
Time: 0.3 sec  
Frame: (a)



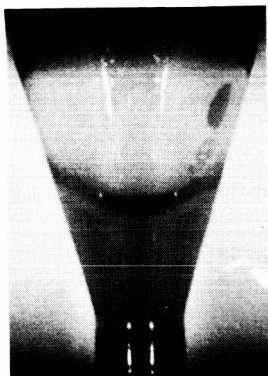
0.5 sec  
(b)



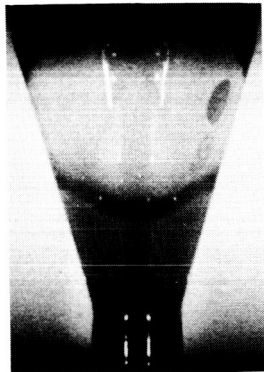
0.7 sec  
(c)



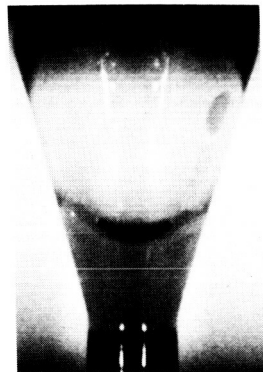
0.9 sec  
(d)



1.1 sec  
(e)



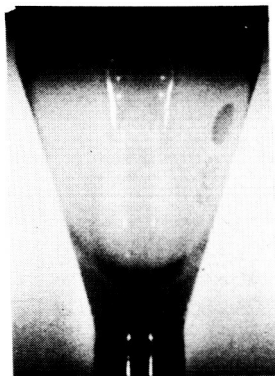
1.3 sec  
(f)



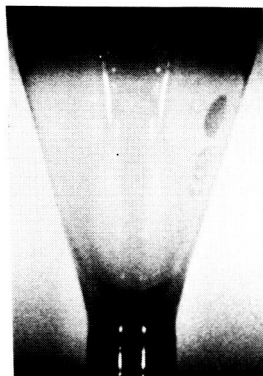
1.5 sec  
(g)



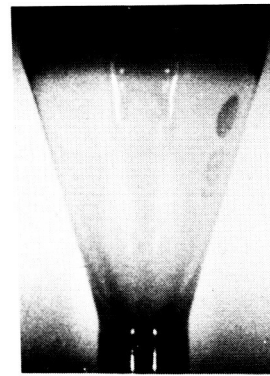
1.7 sec  
(h)



1.9 sec  
(i)



2.1 sec  
(j)



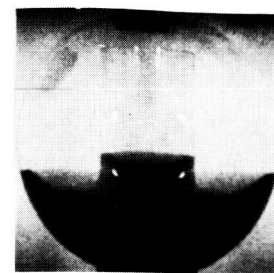
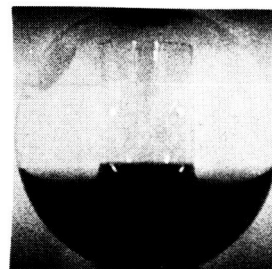
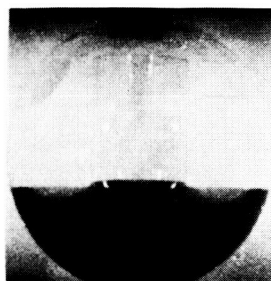
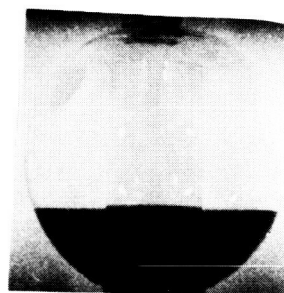
2.2 sec  
(k)

C-63779

Figure 27. - Drop-tower zero-gravity test of liquid discharge from 125-milliliter cone filled 90 percent with ethyl alcohol.

DECLASSIFIED  
CONFIDENTIAL

DECLASSIFIED  
CONFIDENTIAL



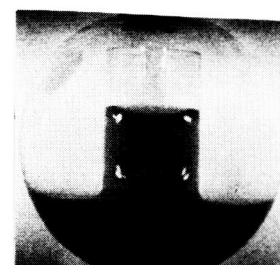
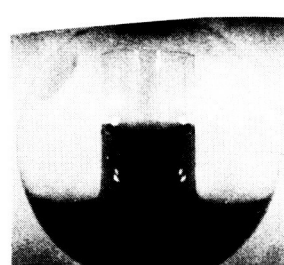
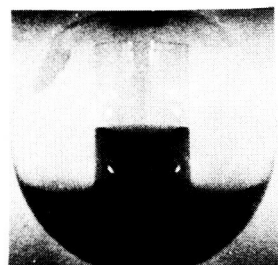
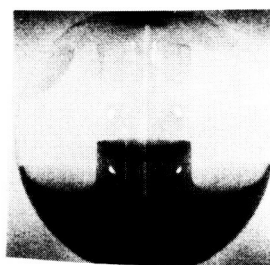
Time:  
Frame:

(a)

0.1 sec  
(b)

0.3 sec  
(c)

0.5 sec  
(d)

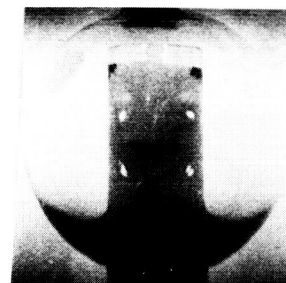
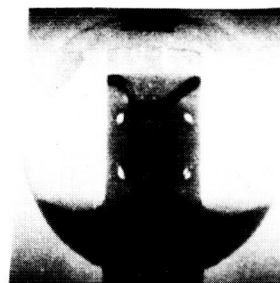
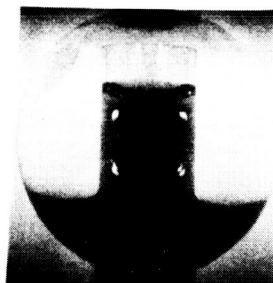
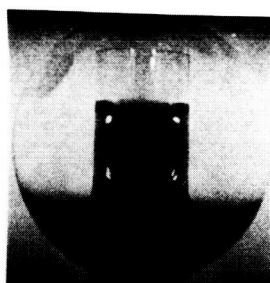


0.7 sec  
(e)

0.9 sec  
(f)

1.1 sec  
(g)

1.3 sec  
(h)

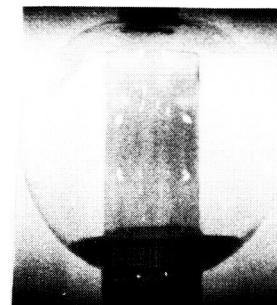
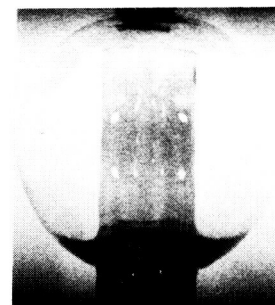
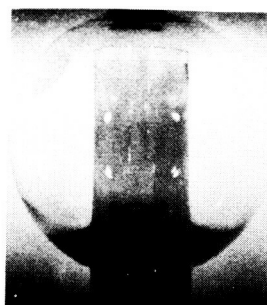
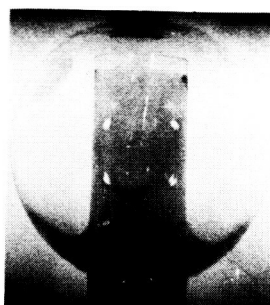


1.5 sec  
(i)

Start discharge  
1.7 sec  
(j)

1.8 sec  
(k)

1.9 sec  
(l)



2.0 sec  
(m)

2.1 sec  
(n)

2.2 sec  
(o)

2.3 sec  
(p)

C-63780

Figure 28. - Drop-tower zero-gravity test of liquid discharge from 100-milliliter sphere with capillary control device. Sphere 20 percent filled with ethyl alcohol.

DECLASSIFIED  
CONFIDENTIAL

DECLASSIFIED  
CONFIDENTIAL

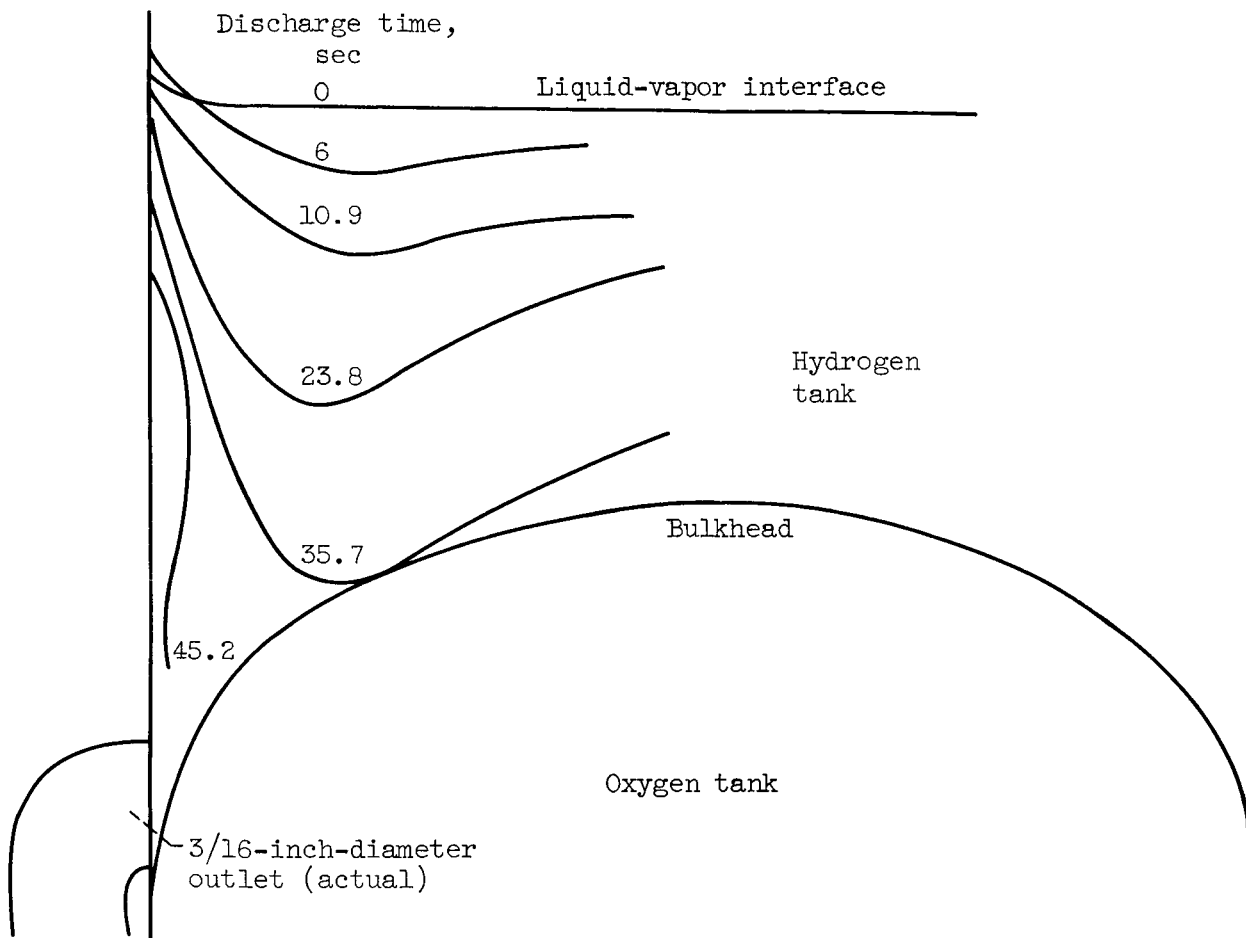


Figure 29. - Drop-tower zero-gravity test of 30-percent filled model tank (discharge time scaled to 10-foot-diameter tank, ref. 41) showing vapor pull-through during outflow. Outlet velocity, 11 feet per second.

DECLASSIFIED  
CONFIDENTIAL